**Loss of C/EBP-β LIP drives cisplatin resistance in malignant pleural mesothelioma**

Elsevier Editorial System(tm) for Lung Cancer

Manuscript Draft

Manuscript Number: LUNGCANCER-D-17-01176R1

Title: Loss of C/EBP-β LIP drives cisplatin resistance in malignant pleural mesothelioma

Article Type: Research paper

Keywords: malignant pleural mesothelioma; CAAT/enhancer binding protein; cisplatin resistance; endoplasmic reticulum stress; immunogenic cell death

Corresponding Author: Dr. Chiara Riganti, MD

Corresponding Author's Institution: University of Torino

First Author: Joanna Kopecka

Order of Authors: Joanna Kopecka; Iris C Salaroglio; Luisella Righi; Roberta Libener; Sara Orecchia; Federica Grosso; Vladan Milosevic; Preeta Ananthanarayanan; Luisa Ricci; Enrica Capelletto; Monica Pradotto; Francesca Napoli; Massimo Di Maio; Silvia Novello; Menachem Rubinstein; Giorgio V Scagliotti; Chiara Riganti, MD

Abstract: Objectives. Cisplatin-based chemotherapy is moderately active in malignant pleural mesothelioma (MPM) due to intrinsic drug resistance and to low immunogenicity of MPM cells. CAAT/enhancer binding protein (C/EBP)-β LIP is a pro-apoptotic and chemosensitizing transcription factor activated in response to endoplasmic reticulum (ER) stress.
Materials and methods. We investigated if LIP levels can predict the clinical response to cisplatin and survival of MPM patients receiving cisplatin-based chemotherapy. We studied the LIP-dependent mechanisms determining cisplatin-resistance and we identified pharmacological approaches targeting LIP, able to restore cisplatin sensitiveness, in patient-derived MPM cells and animal models. Results were analyzed by a one-way analysis of variance test.
Results. We found that LIP was degraded by constitutive ubiquitination in primary MPM cells derived from patients poorly responsive to cisplatin. LIP ubiquitination was directly correlated with cisplatin chemosensitivity and was associated with patients' survival after chemotherapy. Overexpression of LIP restored cisplatin's pro-apoptotic effect by activating CHOP/TRB3/caspase 3 axis and up-regulating calreticulin, that triggers MPM cell phagocytosis by dendritic cells and expanded autologous anti-tumor CD8+CD107+T-cytotoxic lymphocytes. Proteasome inhibitor carfilzomib and lysosome inhibitor chloroquine prevented LIP degradation. The triple combination of carfilzomib, chloroquine and cisplatin increased ER stress-triggered apoptosis and immunogenic cell death in patients' samples, and reduced tumor growth in cisplatin-resistant MPM preclinical models.
Conclusion. The loss of LIP mediates cisplatin resistance, rendering LIP a possible predictor of cisplatin response in MPM patients. The association of proteasome and lysosome inhibitors reverses cisplatin resistance by restoring LIP levels and may represent a new adjuvant strategy in MPM treatment.

*Cover Letter

Torino, 12 March 2018

To the kind attention of

Professor Ross A Soo

Associated Editor

Lung Cancer

Dear Professor Soo,

attached please find our revised manuscript # LUNGCANCER-D-17-01176.

On the basis of the Reviewers' criticisms, we extensively changed text an Figures. We added two new Supplementary Figures and one new Supplementary Table. We would like to thank the Reviewers for their thoughtful comments, which have improved the manuscript substantially.

We hope that the revised version of the manuscript will be considered worthy of publication in Lung Cancer.

All the authors have read and approved the submission of the manuscript.

The manuscript has not been published previously and is not being considered concurrently by another journal.

The authors also declare that there are no conflicts of interest.

Sincerely yours,

Chiara Riganti

**Corresponding author:** Dr. Chiara Riganti, Department of Oncology, University of Torino, via Santena 5/bis, 10126 Torino, Italy; phone: +39116705857; fax: +39116705845; email: chiara.riganti@unito.it

**Reply to Reviewers**

**Reply to Reviewer 1**

*Reviewer #1: The authors examined the importance of the biomarker of "C/EBP-beta LIP" in predicting cisplatin resistance and patient prognosis with malignant pleural mesothelioma. A lot of experiments, using a variety of techniques have been carried out in this body of work and I commend the authors for that. The main findings were the loss of LIP mediates cisplatin resistance and preclinically, proteasome and lysosome inhibitors reverse cisplatin resistance by restoring LIP levels. If this conclusion is validated by other groups, it could be an important advance in malignant mesothelioma, given the limited treatment options and the generally grim prognosis.*

*The paper is generally well written and the discussion is clear. However, given the audience of Lung Cancer (the journal) is generally clinical, I think more simple explanations may be needed in the results part to make it easier to understand for the clinical audience.*

*1) My main concern is that perhaps the key findings do not support the conclusion of the paper and I think the authors will need to explain this a lot better. I refer to the results in Figure 1. This part of the experiments plays a key role and forms the rationale for the rest of the experiments and overall story.*

*- Figure 1 legend (line 465, page 20) states, Arrow, upper panel. However, there is no arrow in figure b, upper panel. So I assume it should be middle panel as there is an arrow stating UQ-C/EBP-beta LIP*

*- If my assumption is correct, the western blot shows that the highest ubiquitinated LIP appears to be in patient 7, 8, 9 which represents the sarcomatous patients. If this is true, those patients appear to have low survival (Supplementary table 2; stating*

*survival of 6, 10, 5 months respectively)*

*- This is then in direct contradiction to figure 1d, which is meant to show LIP ubiquitination level. The Kaplan meier curve would suggest that LIP high (high LIP ubiquitination) have longer survival - contradicting to the data in figure 1b and supplementary table 2)*

We apologize for the mistake in the legend of Figure 1. The arrow refers to the middle panel, as the Reviewer noted. We corrected the legend in the revised version.

It is true that the highest ubiquitinated C/EBP-β LIP appears to be in patients 7, 8, 9, i.e. the patients with sarcomatous histotype and the lowest survival.

Ubiquitinated LIP is a typical sign of its degradation: when a high ubiquitination signal is detected (Figure 1b, middle panel), C/EBP-β LIP protein is low, owing to its continuous degradation via proteasome and lysosome [Li Y et al, J. Biol. Chem. 283 (2008) 22443-22456; Chiribau C et al, Mol. Cell. Biol. 30 (2010) 3722-3731; Riganti C et al, J. Natl. Cancer Inst. 107 (2015) piidjv046]. This event, that occurs in most ubiquitinated proteins [Dikic I, Annu. Rev. Biochem. 86 (2017) 193-224], explains the very low (patient 8) or absent (patient 7, 9) detection of C/EBP-β LIP (Figure 1b, upper panel). Patients with high ubiquitinated C/EBP-β LIP correspond to the category "LIP low" patients of the old Figure 1d. These patients (patients number 3, 4, 7, 8, 9) had low survival.

We apologize for not having clearly explained these correlations. We modified Results (page 10, line 226; page 11, line 230), Discussion (page 14, line 329), Figure 1f (the old Figure 1d) and its legend to make this point clearer. We added two new references.

*- Line 470, page 20, should it be Figure 1b, rather than Figure 1a?*

We corrected the figure legend.

- Line 471, page 20, should it be Figure 1b again, rather than Figure 1a?

We corrected the figure legend.

- *Fiugre 1c itself, there is an arrow of HMC pointing to very low IC50. This is a little unusual, as my understanding is that generally normal mesothelial cells tend not to be sensitive to cisplatin at all. Please explain*.

We agree that the $IC_{50}$ in immortalized commercially available cell lines such as Met-5A is significantly higher than the $IC_{50}$ found in the present work and comparable to the $IC_{50}$ observed in malignant pleural mesothelioma (MPM) cells. In the present work, however, we used primary human mesothelial cells (HMC) that undergo to a rate of spontaneous apoptosis of about 10% cells at each passage when put in culture. Although HMC were used before passage number 4 to avoid an excessive population of apoptotic cells in the cultures and we verified that the cell viability (measured by Trypan Blue staining) before each experiments was $\geq$ 85%, we cannot exclude that the intrinsically-occurring apoptosis synergized with the pro-apoptotic effects induced by cisplatin, producing such low $IC_{50}$. The mean $IC_{50}$ to cisplatin for the three HMC samples was 3.47 $\pm$ 1.96 µM. This data is in line with previously data on published on primary HMC [Salaroglio IC et al, Oncotarget 6 (2015) 1128-1142].

*However, I may have mis-interpreted the results due to the ?mislabelling of figure 1 legend. Nevertheless, the authors need to correct the legend and explains this better.*

*It would make more sense that ubiquitination LIP high would be predictive of low survival (as this would represent low LIP itself) and that the hypothesis of low LIP*

*predicting for cisplatin resistance would make more sense. It would then also pave the way for the rest of the paper, which is trying to increase t he LIP level to reverse the cisplatin resistance.*

We apologize again for the mislabeling of Figure 1 that led to data mis-interpretation. As stated before, we corrected the Figure and modify the text to clarify the key hypothesis of our work: "high LIP ubiquitination, i.e. low LIP level, means cisplatin resistance".

*There are other more minor points that I think authors need to address to strengthen the paper:*

*1. Figure 2a: did the authors look at what happens to Ubiquitination of LIP? Did it reduce corresponding to an increase of LIP*?

We thanks the Reviewer for the interesting observation. We measured the ubiquitination of LIP on the same extracts used in Figure 2a. The results are shown in the new Supplementary Figure 1. Although cisplatin slightly increased LIP amount, in consequence of the cisplatin-induced ER stress [Mandic A et al, J. Biol. Chem. 278 (2003) 278 9100-9106], it did not significantly change the basal rate of LIP ubiquitination compared to untreated cells (Supplementary Figure 1a, Supplementary Table 4b), meaning that induced LIP is ubiquitinated and destroyed by the cell. This explains the absent activation of pro-apoptotic LIP/CHOP/TRB3/caspase 3 axis and the consequent resistance to cisplatin (Figure 2). The ratio ubiquitinated LIP/total LIP, calculated by densitometric analysis, was unchanged compared to untreated cells (Supplementary Figure 1b). Also in LIP-transduced cells, LIP protein underwent ubiquitination (Supplementary Figure 1a, Supplementary Table 4b). However, the ratio between ubiquitinated LIP/total LIP was decreased in this case (Supplementary

Figure 1b). This trend suggests that the excess of exogenous LIP, as it occurs in LIP-transduced cells, likely saturates the maximal ubiquitination capacity of MPM cells. Therein, in this case a significant amount of LIP remains not-ubiquitinated and triggers the pro-apoptotic CHOP/TRB3/caspase 3 axis (Figure 2). This effect was particularly pronounced in LIP-transduced cells treated with cisplatin (Figure 2a): the sum of endogenous LIP induced by cisplatin and exogenous LIP produced by the transfection with a LIP-overexpressing vector results in huge increase of not-ubiquitinated LIP, allowing the induction of LIP-dependent apoptosis.
We reported these data in the Results (page 11, line 252) and commented them in the Discussion (page 16, line 360). We modified Supplementary materials accordingly.

2. *Figure 2d: I note that the cells with treated with cisplatin with a concentration of 25microM. For MPM1, I note that the IC50 was ~28microM as per Supplementary Table 3). Therefore, the Pt treated plate for MPM1 in figure 2d does not seem to represent an IC50 of 28 (if treated by Pt concentration of 25). The plates for MPM 7 in figure 2d makes sense with IC50 for MPM 7 being ~71)*
$IC_{50}$ (Supplementary Table 3) was calculated by performing the Neutral Red staining, a quantitative assay that is more sensitive than crystal violet staining, used in Figure 2d. Crystal violet staining was used as a qualitative assay. The different sensitivity of the techniques - together with the poor ability of primary MPM cells to uptake crystal violet in an homogeneous way compared to other rapidly dividing cell lines - may explain the apparent differences between the $IC_{50}$ calculated in Supplementary Table 3 and the image of the scanned well in Figure 2d. To give a more quantitative measure of the staining, we dissolved crystal violet dye with 1% v/v acetic acid and we read the absorbance of each well at 570 nm (HT Synergy 96-well microplate

reader, Bio-Tek Instruments, Winoosky, VT).The mean of absorbance units of untreated cells was considered 100%; the absorbance units of the other experimental conditions were expressed as percentage towards untreated cells. The results of the quantification are shown in the right panel of Figure 2d, and demonstrated that 25 µM cisplatin reduced cell viability in MPM1 to around 63.4%±. 7.12, that is not significantly different from the $IC_{50}$ calculated in Supplementary Table 3.
We modified Materials and methods (page 7, line 150) and Figure 2 accordingly.

3. *Graphic quality could be improved in Figure 4C and Figure 6d. The scale in the figures seems a little inconsistent?*
We improved the quality of the Figure 4c and 6d. We apologized for the copy-and-paste mistake reporting the length of the scale bar in the figure legends. We corrected it.

4. *Figure 4b: it seems that cisplatin alone also increase LIP somewhat. Please comment*.
One of the mechanisms of cisplatin-induced toxicity is the induction of ER stress-mediated apoptosis [Mandic A et al, J. Biol. Chem. 278 (2003) 278 9100-9106] that is mediated by LIP activation [Riganti C et al, J. Natl. Cancer Inst. 107 (2015) piidjv046]. In human MPM cells we indeed observed a small increase in LIP in cells treated with cisplatin (see for instance MPM1 cell extracts of Figure 2a), likely as a consequence of a low level of ER stress induced by the drug. In solid tumors, ER stress often occurs as a consequence of hypoxia or nutrient t shortage [Chevet E et al, Cancer Discov. 5 (2015) 586-597]. These conditions are sufficient to induce LIP activation [Meir O et al, PLoS One. 5 (2010) e9516]. The ER tress dependent on

tumor environment and the ER stress elicited by cisplatin can produce the small induction of LIP observed in tumor extracts of Figure 4b. However, this induction of LIP was insufficient to trigger ER-dependent apoptosis, as demonstrated by the absent intratumor activation of CHOP and caspase 3 (Figure 4c).
We added a comment in the Discussion (page 16, line 377) on this point.

5. *Figure 5d: Did the authors examine what happens with PT (cisplatin) alone? Also what happens with ubiquitination LIP? Did it reduce as expected with increased LIP*?
The effects of cisplatin treatment alone have been already reported in Figure 2a: to avoid redundancy, we did not report these data again in Figure 5d. We added a sentence in the legend of Figure 5 stating this.
We measured the ubiquitination of LIP on the same extracts of Figure 5d. The results are reported in the new Supplementary Figure 7. The treatment with carfilzomib and chloroquine, alone or in combination, increased the accumulation of ubiquitinated LIP in whole cell extracts compared to untreated cells (Supplementary Figure 7a, Supplementary Table 4c). The same increase in ubiquitinated LIP was detected in cells treated with the triple combination carfilzomib + chloroquine + cisplatin. Since carfilzomib and chloroquine inhibit proteasome and lysosome, respectively - that act downstream the ubiquitination system - they prevent the degradation of ubiquitinated proteins by proteasome and lysosome [Dikic I, Annu. Rev. Biochem. 86 (2017) 193-224]. However, the ratio between ubiquitinated LIP/total LIP is lowered in carfilzomib- and chloroquine-treated cells, in particular in the combination treatments carfilzomib + chloroquine or carfilzomib + chloroquine + cisplatin (Supplementary Figure 7b). This trend suggests that carfilzomib and chloroquine produce an “action mass”-like effect: by blocking the degradation of ubiquitinated LIP via proteasome

and lysosome, the drugs increase the amount of ubiquitinated LIP to a level saturating the ubiquitination capacity of MPM cells (see also the reply to minor point 1). This saturation ultimately results in the accumulation of not-ubiquitinated LIP that triggers the CHOP/TRIB3/caspase 3 pro-apoptotic pathway (Figure 5d).
We reported these data in the Results section (page 13, line 303) and commented them in the Discussion (page 17, line 403). We modified Supplementary materials accordingly.

6. *Figure 6a: What about cisplatin treated alone?*
The effects of cisplatin treatment alone have been reported in Figure 2c: to avoid redundancy, we did not report the data in Figure 6a. We added a sentence in the legend of Figure 6 stating this.

7. *Did the MPM patients 1 to 9 receive any other treatments post cisplatin based therapy? If so, would progression free survival (PFS) or response rate (RR) be a more appropriate endpoint to look at rather than OS, as OS may be confounded by subsequent treatment effects?*
The patients selected for this study received in most case second-line treatments after cisplatin + pemetrexed first-line chemotherapy. We reported the treatment scheme in the Supplementary Table 2, along with the progression free survival.
Following the Reviewer's suggestions, we evaluated the progression free survival as end-point. The results are reported in the new Figure 1e and indicated a still significant difference between the "LIP low" and the "LIP high" patient groups.
We modified the Results (page 11, line 230) and Discussion (page 15, line 338) sections, and the legend of Figure 1 accordingly.

*Overall, I think the potential for use of a FDA approved treatment in combination with cisplatin would represent an important advance in the treatment of MPM. The authors will need to discuss the above comments more clearly*

We thanks the Reviewer for the useful comments, that substantially improved the manuscript. We hope to have exhaustively addressed all the comments throughout the manuscript.

**Reply to Reviewer 2**

*Reviewer #2: This manuscript focused on the involvement of LIP, an isoform of the transcription factor c/EBP-beta, in the resistance to cisplatin of malignant pleural mesothelioma (MPM). This manuscript focused on the involvement of LIP, an isoform of the transcription factor c/EBP-beta, in the resistance to cisplatin of malignant pleural mesothelioma (MPM). The authors observed that MPM cell lines have lower expression of LIP than normal mesothelial cells linked to higher ubiquitination of this protein. They also found a correlation between LIP ubiquitination and cisplatin chemosensitivity of MPM cell lines and patients overall survival. Robust molecular functional studies demonstrate that LIP re-expression increase cisplatin sensitivity. Convincing in vitro and in vivo experiments show that LIP re-expression also led to cisplatin-induced apoptosis and immunogenic cell death. Proteasome and lysosome inhibitors restore LIP expression in MPM cells and also sensitizes MPM cells to cisplatin by increasing cisplatin-induced apoptosis and inducing immunogenic cell death.*

*1. The authors need to be more cautious in the abstract. They stated that "LIP levels*

*were directly correlated with cisplatin chemosensitivity and were associated with patients' survival after chemotherapy". They should precise that it is LIP ubiquitination, which is correlated. Furthermore, the statement about the "low immunogenicity of MPM cells" needs to be relativized based on published data. Overall, they should moderate some of their statement especially for the link between LIP ubiquitination and patient overall survival that should be validated in tumor samples from patients*.

As suggested we modified the Abstract (page 2 line 44).

We better defined the “immune-evasive” attitude of MPM cells (Introduction; page 5, lines 82 and 90) and we added new references reporting the molecular mechanisms at the basis of the immune-suppressive environment and the low antigenicity of MPM cells.

We recognize that our preliminary data on the possible role of LIP ubiquitination as predictor of clinical response to cisplatin and survival must be validated in a larger cohort of tumor samples from patients. We modified the Discussion section (page 15, line 347; page 18, line 422) accordingly.

*2. The authors found a correlation between cisplatin IC50 and LIP ubiquitination level, but not LIP protein expression. Based on data showed on Figure 2B, it seems there are no correlation between LIP expression and LIP ubiquitination level. The authors should at least address this point in the discussion. They also need to indicate, in a supplementary table, the LIP ubiquitination level, quantified from the western blot, in each cell line, for a better understanding*.

Since the Figure 2b does not contained immunoblot analysis of total LIP or ubiquitinated LIP; we hypothesized that the Reviewer referred to Figure 1b.

We apologize for not having clearly explained in the text that there was a correlation between ubiquitinated LIP and $IC_{50}$ of cisplatin. We clarified and addressed this point in the Discussion (page 15, line 335). Moreover, we included the quantification of the ratio between ubiquitinated LIP/total LIP reported in Figure 1b, calculated by densitometric analysis (figure 1 c in the revised version). We modified the Results section (page 10, line 226) and the legend of Figure 1 accordingly.

As suggested, we provided the quantification of the ubiquitinated LIP of Figure 1b in the new Supplementary Table 4s. Since the Reviewer 1 asked to investigate the ubiquitination level of LIP in the extracts of Figure 2a and 5d (reported in the Supplementary Figure 1 and 7), we included the quantification of ubiquitinated LIP also for these experimental sets in the Supplementary Table 4b-c. We commented the results of these quantification in the Discussion (page 15, line 335; page 16, line 360; page 17, line 403).

## Highlights

- C/EBP-β LIP loss correlates with poor response to cisplatin in mesothelioma patients

- C/EBP-β LIP loss is due to its constitutive ubiquitination and degradation

- Lack of C/EBP-β LIP prevents cisplatin-induced apoptosis and immunogenic cell death

- Proteasome and lysosome inhibitors restoring C/EBP-β LIP rescue cisplatin efficacy

# Loss of C/EBP-β LIP drives cisplatin resistance in malignant pleural mesothelioma

Joanna Kopecka[a,*], Iris C. Salaroglio[a,*], Luisella Righi[b], Roberta Libener[c], Sara Orecchia[c], Federica Grosso[d], Vladan Milosevic[a], Preeta Ananthanarayanan[a], Luisa Ricci[a], Enrica Capelletto[e], Monica Pradotto[e], Francesca Napoli[b], Massimo Di Maio[f], Silvia Novello[e], Menachem Rubinstein[g], Giorgio V. Scagliotti[e,*] , Chiara Riganti[a,*]

[a] Department of Oncology, University of Torino, via Santena 5/bis, 10126, Torino, Italy

[b] Pathology Unit, Department of Oncology at San Luigi Hospital, University of Torino, Regione Gonzole 10, 10043, Orbassano, Italy

[c] Pathology Division, S. Antonio and Biagio Hospital, Spalto Marengo, 15121, Alessandria, Italy

[d] Oncology Division, S. Antonio and Biagio Hospital, Spalto Marengo, 15121, Alessandria, Italy

[e] Thoracic Unit and Medical Oncology Division, Department of Oncology at San Luigi Hospital, Regione Gonzole 10, University of Torino, Orbassano, Italy

[f] Medical Oncology Division, Department of Oncology at Mauriziano Hospital, Largo Filippo Turati 62, 10128, University of Torino, Italy

[g] Department of Molecular Genetics, The Weizmann Institute of Science, Herzl Street 234, 76100, Rehovot, Israel

***** These authors equally contributed to the work

**Authors email addresses:** JK: joanna.kopecka@unito.it; ICS: irischiara.salaroglio@unito.it; LR: luisella.righi@unito.it; RL: rlibener@ospedale.al.it; SO: sorecchia@ospedale.al.it; FG: fgrosso@ospedale.al.it; VM: vladan.milosevic@unito.it; PA: preeta.ananthanarayanan@unito.it; LRic: luisa.ricci@gmail.com; EC: enrica.capelletto@gmail.com; MP: monica.pradotto@unito.it; FN: francesca.napoli@unito.it; MDM: massimo.dimaio@unito.it; SN: silvia.novello@unito.it; MR:

menachem.rubinstein@weizmann.ac.il; GVS: giorgio.scagliotti@unito.it; CR: chiara.riganti@unito.it

**Corresponding author**: Dr. Chiara Riganti, Department of Oncology, University of Torino, via Santena 5/bis, 10126, Torino, Italy; phone: +390116705857; fax: +390116705845; email: chiara.riganti@unito.it

**Abstract**

**Objectives.** Cisplatin-based chemotherapy is moderately active in malignant pleural mesothelioma (MPM) due to intrinsic drug resistance and to low immunogenicity of MPM cells. CAAT/enhancer binding protein (C/EBP)-β LIP is a pro-apoptotic and chemosensitizing transcription factor activated in response to endoplasmic reticulum (ER) stress.

**Materials and methods**. We investigated if LIP levels can predict the clinical response to cisplatin and survival of MPM patients receiving cisplatin-based chemotherapy. We studied the LIP-dependent mechanisms determining cisplatin-resistance and we identified pharmacological approaches targeting LIP, able to restore cisplatin sensitiveness, in patient-derived MPM cells and animal models. Results were analyzed by a one-way analysis of variance test.

**Results.** We found that LIP was degraded by constitutive ubiquitination in primary MPM cells derived from patients poorly responsive to cisplatin. LIP ubiquitination was directly correlated with cisplatin chemosensitivity and was associated with patients' survival after chemotherapy. Overexpression of LIP restored cisplatin's pro-apoptotic effect by activating CHOP/TRB3/caspase 3 axis and up-regulating calreticulin, that triggers MPM cell phagocytosis by dendritic cells and expanded autologous anti-tumor $CD8^+CD107^+$T-cytotoxic lymphocytes.

Proteasome inhibitor carfilzomib and lysosome inhibitor chloroquine prevented LIP degradation. The triple combination of carfilzomib, chloroquine and cisplatin increased ER stress-triggered

apoptosis and immunogenic cell death in patients' samples, and reduced tumor growth in cisplatin-resistant MPM preclinical models.

**Conclusion.** The loss of LIP mediates cisplatin resistance, rendering LIP a possible predictor of cisplatin response in MPM patients. The association of proteasome and lysosome inhibitors reverses cisplatin resistance by restoring LIP levels and may represent a new adjuvant strategy in MPM treatment.

**Highlights**

- C/EBP-β LIP loss correlates with poor response to cisplatin in mesothelioma patients
- C/EBP-β LIP loss is due to its constitutive ubiquitination and degradation
- Lack of C/EBP-β LIP prevents cisplatin-induced apoptosis and immunogenic cell death
- Proteasome and lysosome inhibitors restoring C/EBP-β LIP rescue cisplatin efficacy

**Keywords:** malignant pleural mesothelioma; CAAT/enhancer binding protein; cisplatin resistance; endoplasmic reticulum stress; immunogenic cell death

**Abbreviations:** ANOVA, analysis of variance; ATF6, activating transcription factor 6; C/EBP, CAAT/enhancer binding protein; IRE1, inositol-requiring enzyme 1; CHOP/GADD153; C/EBP homologous protein/growth arrest/DNA damage inducible 153; CEA, carcino-embrionic antigen; ChIP, chromatin immunoprecipitation; DC, dendritic cells; ER, endoplasmic reticulum; EMA, epithelial membrane antigen; EIF2AK3/PERK, eukaryotic translation initiation factor-2α kinase 3; FBS, fetal bovine serum; ICD, immunogenic cell death; HMC, human mesothelial cells; MPM, malignant pleural mesothelioma; OS: overall survival; qRT-PCR, quantitative Real Time-PCR; PFS: progression free survival; SPSS, Statistical Package for Social Science; TBS, Tris-buffered

saline; TRB3, *tribbles*-related protein 3; UPN, Unknown Patient Number; WT1, Wilms tumor-1 antigen

## 1. Introduction

Malignant pleural mesothelioma (MPM), an asbestos-related cancer, is usually diagnosed at advanced stage, when chemotherapy - based on cisplatin associated with pemetrexed or raltitrexed - is the only available therapeutic option. [1,2]. The success of chemotherapy is limited by the intrinsic chemoresistance [1] and immune-evasive nature of MPM. Such immune-evasive microenvironment in MPM relies on the presence of immune-suppressive/immune-tolerant cells in the MPM [3, 4], on the high levels of immune-suppressive immune-checkpoints on both MPM cells and surrounding T-lymphocytes [5, 6], on the low amount of tumor-associated antigens of MPM cells [7], due to its low mutational burden [8].

In sensitive cells, cisplatin induces DNA damage, hampers DNA repair [9] and elicits nuclear-independent effects, such as dispersal of Golgi apparatus [10] and apoptosis induced by endoplasmic reticulum (ER) stress [11]. Upon ER stress, cancer cells expose on their surface the "eat-me" signal calreticulin, leading to dendritic cells (DC)-mediated phagocytosis and activation of autologous anti-tumor cytotoxic $CD8^+$T-lymphocytes [12]. This process is known as immunogenic cell death (ICD) [12]. MPM cells however do not translocate calreticulin from ER to surface [13, 14], resulting ICD-refractory. This is an additional mechanism explaining the low immunogenicity of MPM cell.

Solid tumors respond to chemotherapy-induced ER stress by activating adaptation and survival pathways if the stress is limited, or pro-apoptotic pathways if the stress persists [15, 16]. The ER stress-induced transcription factor CAAT/enhancer binding protein (C/EBP)-β is involved in both responses. At the early ER stress phase, the pro-survival isoform C/EBP-β LAP is produced. Upon prolonged ER stress, the isoform C/EBP-β LIP (LIP) is formed and activates C/EBP homologous protein/growth arrest/DNA damage inducible 153 (CHOP/GADD153) protein, which promotes apoptosis by activating *tribbles*-related protein 3 (TRB3) and caspase 3 [17-20]. At the present there are no data available about gene alterations (mutation, amplification or deletion) in the 87 MPM evaluated by the Tissue Cancer Genome Atlas (https://cancergenome.nih.gov), nor about the

expression of C/EBP-β LAP/LIP isoforms in MPM, according to Protein Tissue Atlas (http://www.proteinatlas.org).

We recently reported that chemoresistant tumors lack LIP, because of its constitutive ubiquitination. LIP loss mediates chemoresistance by increasing the expression of the drug efflux transporter P-glycoprotein and by preventing the ER stress-dependent pro-apoptotic response [12].

Here, we investigated if LIP mediates the resistance to cisplatin in MPM. We identified clinically feasible pharmacological strategies that restore the sensitivity of MPM to cisplatin by preventing LIP degradation.

## 2. Materials and methods

**2.1.Chemicals.** Cell culture plastic ware were obtained from Falcon (Becton Dickinson, Franklin Lakes, NJ). Electrophoresis reagents were obtained from Bio-Rad Laboratories (Hercules, CA). Carfilzomib was purchased from Biorbyt Ltd. (Cambridge, UK) and torin 1 was from Selleckchem (Munich, Germany). The protease inhibitor cocktail set III was obtained from Millipore (Billerica, MA). Unless specified otherwise, all reagents were purchased from Sigma Chemicals Co (St. Louis, MO).

**2.1.Cells.** Primary human mesothelial cells (HMC) were isolated from three patients with pleural fluid secondary to congestive heart failure, with no history of a malignant disease. Nine primary human MPM samples (3 epithelioid MPM, 3 biphasic MPM, 3 sarcomatous MPM) were obtained from diagnostic thoracoscopies. Histological and clinical features are shown in Supplementary Tables 1-2. All patients, identified with Unknown Patient Numbers (UPN), received 5 cycles of cisplatin 75 mg/m$^2$ every 21 days. Tissue was digested in medium containing 1 mg/ml collagenase and 0.2 mg/ml hyaluronidase for 1 h at 37°C. Cells were seeded in culture and used within passage 6. The Ethical Committee of Biological Bank of Mesothelioma, S. Antonio e Biagio Hospital, Alessandria, Italy, and San Luigi Gonzaga Hospital, Orbassano, Italy, approved the study (#9/11/2011; #126/2016). Murine AB1 cells were purchased from Sigma Chemicals Co. Cells were

grown in Ham's F10 nutrient mixture medium (primary HMC/MPM cells) or DMEM (AB1 cells), supplemented with 10% v/v fetal bovine serum, 1% v/v penicillin-streptomycin.

**2.3.Quantitative Real Time-PCR (qRT-PCR).** RNA was extracted and reverse-transcribed using the iScript™ cDNA Synthesis Kit (Bio-Rad Laboratories). qRT-PCR was performed using IQ™ SYBR Green Supermix (Bio-Rad Laboratories). The same cDNA preparation was used for measuring genes of interest and the housekeeping gene *S14*. Primer sequences were designed using qPrimerDepot software (http://primerdepot.nci.nih.gov/). Relative gene expression levels were calculated using Gene Expression Quantitation software (Bio-Rad Laboratories).

**2.4.Immunoblotting.** Protein or tumor extracts (20 μg) were subjected to SDS-PAGE and probed with the following antibodies: C/EBP-β (directed against the common C-terminus of LIP and LAP, Santa Cruz Biotechnology Inc., Santa Cruz, CA), CHOP/GADD153 (Abcam, Cambridge, UK), TRB3 (Proteintech, Chicago, IL), caspase-3 (GeneTex, Hsinhu City, Taiwan), β-tubulin (Santa Cruz Biotechnology Inc.). To detect ubiquitinated C/EBP-β, 100 μg protein extracts were immuno-precipitated overnight with the anti-C/EBP-β antibody, using 25 μl of PureProteome Magnetic Beads (Millipore). Immunoprecipitated samples were then probed with an anti-mono/polyubiquitin antibody (Axxora). Blotting was followed by the peroxidase-conjugated secondary antibody. The membranes were washed with Tris-buffered saline/Tween 0.01% v/v and proteins were detected by enhanced chemiluminescence. Band density was calculated using ImageJ software (http://www.rsb.info.nih.gov/ij/).

**2.5.Cell viability and growth**. Cell viability with neutral red staining and crystal violet staining were performed as reported [20]. $IC_{50}$ was calculated with the CompuSyn software (http://www.combosyn.com). Quantitation of crystal violet staining was performed by dissolving crystal violet with 1% v/v acetic acid and reading the absorbance of each well at 570 nm (HT Synergy 96-well microplate reader, Bio-Tek Instruments, Winoosky, VT).The mean absorbance of

untreated cells was considered 100%; the absorbance units of the other experimental conditions were expressed as percentage towards untreated cells.

**2.6.Cell cycle analysis.** $1\times10^4$ cells were harvested, washed with PBS, treated with 0.25 mg/ml RNAse and stained for 15 min with 50 μg/ml propidium iodide. Cell cycle distribution was analyzed by Guava® easyCyte flow cytometer (Millipore, Billerica, MA), using the InCyte software (Millipore).

**2.7.Over-expression of C/EBP-β LAP and LIP.** The pcDNA4/TO expression vectors (Invitrogen Life Technologies, Milan, Italy) for LAP and LIP, produced as reported previously [17], were co-transduced with pcDNA6/TR vector (Invitrogen Life Technologies) in parental cells. Stable TetON clones were generated by selecting cells with 2 μg/ml blasticidin S (Invitrogen Life Technologies) and 100 μg/ml zeocin (InvivoGen, San Diego, CA). LAP and LIP induction was activated by adding 1 μg/ml doxycycline in the culture medium.

**2.8.C/EBP-β LIP silencing.** $2\times10^6$ cells in 0.25 ml serum/antibiotic-free medium were transfected either with non-targeting scrambled siRNA pools or siRNA pools specifically targeting LIP sequence (customized ON-TARGETplus, Dharmacon RNAi Technologies; Dharmacon, Lafayette, CO), employing DharmaFECT 1 reagent (Dharmacon), as per manufacturer's protocol.

**2.9.Chromatin immunoprecipitation (ChIP).** To determine the binding of LAP and LIP to calreticulin promoter we performed ChIP as described [21], using the anti-C/EBP-β antibody directed against the common C-terminus of LAP and LIP. Putative binding sites of C/EBP-β were identified using the Gene Promoter Miner software (http://gpminer.mbc.nctu.edu.tw/). PCR primers were designed using Primer3 software (http://primer3.ut.ee/).

**2.10.Calreticulin expression, phagocytosi and T-lymphocyte activation.** Surface calreticulin was measured by flow cytometry as reported [22]. DC were generated from peripheral blood samples of patients, collected before starting chemotherapy, as previously reported [13]. Phagocytosis assays were performed as detailed in [22]. Active anti-tumor cytotoxic $CD8^+CD107^+$T-lymphocytes,

obtained from autologous T-lymphocytes (co-cultured 10 days with DC after phagocytosis) and isolated with the Pan T Cell Isolation Kit (Miltenyi Biotec., Bergisch Gladbach, Germany), were measured by flow cytometry [13]. The production of IFN-γ in the culture supernatant of $CD8^+$T-cells co-cultured with DC or in the supernatant of tumor-draining lymph nodes - a second parameter of $CD8^+$T-cells cytotoxic activity - was measured with the Human IFN-γ DuoSet Development Kit (R&D Systems, Minneapolis, MN).

**2.11.*In vivo* tumor growth.** $1\times10^7$ AB1 cells expressing LIP upon doxycycline administration in drinking water, mixed with 100 µl Matrigel, were injected subcutaneously (s.c.) in 6-weeks-old female immune-competent or immune-deficient (nude) balb/C mice (Charles River Laboratories Italia, Calco), housed (5 per cage) under 12 h light/dark cycle, with food and drinking provided *ad libitum*. Tumor growth was measured daily by caliper, according to the equation $(LxW^2)/2$, where L=tumor length and W=tumor width. When tumor reached the volume of 50 $mm^3$, animals were randomized and treated as reported in the Figure Legends. Tumor volumes were monitored by caliper and animals were euthanized at day 21 after randomization with zolazepam (0.2 ml/kg) and xylazine (16 mg/kg). The hemocromocytometric analyses were performed with a UniCel DxH 800 Coulter Cellular Analysis System (Beckman Coulter, Miami, FL) on blood collected immediately after sacrificing the mice. Hematochemical parameters were analyzed using the respective kits from Beckman Coulter Inc. Animal care and experimental procedures, according to EU Directive 2010/63, were approved by the Bio-Ethical Committee of the Italian Ministry of Health (#122/2015-PR).

**2.12.Immunohistochemistry and intratumor immune infiltrate analysis**. Tumors were resected and fixed in 4% v/v paraformaldehyde, stained with hematoxylin/eosin or immunostained for CHOP or cleaved(Asp175)-caspase 3 (Cell Signaling Technology Inc., Danvers, MA), followed by a peroxidase-conjugated secondary antibody. Nuclei were counter-stained with hematoxylin. Sections were examined with a Leica DC100 microscope. Excised tumors were digested with 1 mg/ml collagenase and 0.2 mg/ml hyaluronidase (1h at 37°C) and filtered using a 70 µm cell

strainer to obtain a single cell suspension. Infiltrating immune cells were collected by centrifugation on Ficoll-Hypaque density gradient and subjected to immune phenotyping by flow cytometry, using antibodies against CD11c for DC, CD3 and CD8 for T-lymphocytes (Miltenyi Biotec.). Draining lymph nodes were collected, homogenized for 30 s at 15 Hz, using a TissueLyser II device (Qiagen, Hilden, Germany) and centrifuged at 12000 x g for 5 minutes. The supernatant was used to measure the amount of IFN-γ.

**2.13.Proteasome, autophagy and lysosome activity.** Proteasome activity was measured with the Proteasome-Glo™ Cell-Based Assays (Promega Corporation). Autophagy activity was measured using the Autophagy Assay Kit (Sigma Chemicals Co.). The activity of cathepsin L, taken as an index of lysosome activity, was measured as reported [23].

**2.14.Statistical analysis.** All data in the text and figures are provided as means±SD. The results were analysed by a one-way analysis of variance (ANOVA), using Statistical Package for Social Science (SPSS) software (IBM SPSS Statistics v.19). $p<0.05$ was considered significant. Overall survival was defined as the time passed from the starting of cisplatin therapy to the date of death (all patients were dead at the time of analysis). The Kaplan-Meier method was used to calculate overall survival. Log rank test was used to compare the outcome of the two groups. The sample size was calculated with the G*Power software (www.gpower.hhu.de), setting $\alpha \leq 0.05$ and $1-\beta=0.80$.

## 3. Results

### 3.1.LIP is constitutively ubiquitinated in mesothelioma and correlates with cisplatin resistance

*C/EBP-β* mRNA was equally expressed in primary non-transformed HMC and MPM cells (Figure 1a). By contrast, C/EBP-β LAP protein was detected in both HMC and MPM samples, LIP was detectable only in HMC. The absence or very low expression of LIP in MPM was due to its higher ubiquitination: lower was the level of LIP in MPM (*upper panel*, Figure 1b), higher was LIP ubiquitination (*middle panel*, Figure 1b; Figure 1c), suggesting that LIP ubiquitination can be paralleled by its degradation, as it occurs for most ubiquitinated proteins [24] All MPM samples were significantly more resistant to cisplatin *in vitro* compared to HMC (Supplementary Table 3).

Ubiquitinated LIP was directly correlated with the $IC_{50}$ of cisplatin (Figure 1d). LIP ubiquitination was also significantly associated with patients' progression free survival (PFS; Figure 1e) and overall survival (OS; Figure 1f) after cisplatin therapy: median PFS was 2.2 months, median OS was 9 months (Supplementary Table 2) in the top 5 patients (UPN 3, 4, 7, 8, 9) with highest LIP ubiquitination (LIP ubiquitination higher or equal to median value, Supplementary Table 4a). This group was called "LIP low group" in Figure 1e-f, since patient-derived cell had lower levels of LIP protein (Figure 1b, *upper panel*). Median PFS and OS were 5.3 and 16 months respectively (Supplementary Table 2) in the top 4 patients (UPN 1, 2, 5, 6) with lowest LIP ubiquitination (LIP ubiquitination lower or equal to median value, Supplementary Table 4a). This group was defined as "LIP high group" in Figure 1e-f, since patient-derived cells had higher levels of LIP protein (Figure 1b, *upper panel*).

### 3.2.Reconstitution of LIP restores cisplatin-induced cell death by activating ER stress-mediated apoptosis

To investigate whether there was a causal relationship between the loss of LIP and the resistance to cisplatin, we induced overexpression of exogenous LIP in MPM cells (Figure 2a). LIP transduced cells were more sensitive to cisplatin (Supplementary Table 5), activated the pro-apoptotic CHOP/TRB3/caspase 3 axis (Figure 2a), increased the percentage of sub-G1 apoptotic cells, reduced the percentage of cells entering the S-phase (Figure 2b), decreased cell proliferation (Figure 2c-d).

Cisplatin did not activate the LIP/CHOP/TRB3/caspase 3 axis, neither affected cell cycle, nor proliferation, in non-transduced MPM cells, whereas LIP induction restored all these events. The combination "LIP induction+cisplatin treatment" was superior to LIP induction only (Figure 2a-d). Although cisplatin slightly increased LIP amount, it did not change the basal rate of LIP ubiquitination, meaning that the induced LIP was ubiquitinated (Supplementary Figure 1a; Supplementary Table 4b) and subsequently degraded by the cell. The ratio ubiquitinated LIP/total LIP, calculated by densitometric analysis, was unchanged compared to untreated cells

(Supplementary Figure 1b). Also, in LIP-transduced cells, LIP protein underwent ubiquitination (Supplementary Figure 1a; Supplementary Table 4b). However, the ratio ubiquitinated LIP/total LIP was decreased in this case (Supplementary Figure 1b).

### 3.3.LIP triggers immunogenic cell death in mesothelioma cells

As observed above, MPM cells are refractory to ICD mediated by calreticulin [13, 14]. Two predicted binding sites for C/EBP transcription factors are present in calreticulin promoter at position 831-843 and 1302-1313 (Supplementary Figure 2a). The former one contains a CCAAT box motif (Supplementary Figure 2b). To investigate whether C/EBP-β interacts with calreticulin promoter, we used MPM clones constitutively overexpressing LAP or LIP (Figure 3a). Of note, LIP bound the 831-843 site (Figure 3b). LIP-transduced cells increased calreticulin mRNA and surface protein (Figure 3c-d), were easily phagocytized by DC (Figure 3e), expanded autologous activated $CD8^+$ $CD107^+$ T-lymphocytes producing IFN-γ (Figures 3f-g). By contrast, LAP overexpressing cells did not differ from non-transduced MPM samples (Figure 3c-g).

As a proof of concept of the role of LIP in these process, we silenced the exogenously expressed LIP in MPM cells (Supplementary Figure 3a). In LIP-silenced cells calreticulin expression, phagocytosis and antitumor cytotoxic T-lymphocyte expansion were abrogated (Supplementary Figures 3b-d), demonstrating the critical role of LIP as calreticulin inducer and ICD effector in MPM.

### 3.4.LIP expression restores sensitivity to cisplatin and immune-mediated death *in vivo*

To validate the effects of LIP overexpression *in vivo*, we produced doxycycline-inducible LIP clones from AB1 cells (Supplementary Figure 4), a murine mesothelioma cell line syngeneic with balb/C mice. $IC_{50}$ of cisplatin was 91.08 ± 17.18 μM in un-induced AB1 cells, in line with the most cisplatin-resistant human MPM cells (Supplementary Table 3). Accordingly, AB1-tumors were unresponsive to cisplatin when implanted in mice (Figure 4a). Upon induction of LIP (Figure 4b), the tumor growth was reduced in both immune-deficient and immune-competent mice (Figure 4a) and showed increased percentage of tumor cells positive for CHOP and cleaved caspase 3 (Figure

3c), in particular in LIP-induced/cisplatin-treated mice. The antitumor effects of LIP + cisplatin were stronger in immune-competent mice, at least during the early development of MPM (Figure 4a), suggesting that immune system activation plays a significant role in delaying MPM growth. In immune-competent mice, LIP induction increased intratumor infiltrating DC and $CD8^+$ T-lymphocytes, and production of IFN-γ in draining lymph nodes (Figure 4d-f). Cisplatin enhanced all these events in LIP-expressing tumors (Figure 4d-f).

**3.5.LIP undergoes proteasomal and lysosomal degradation**

Since LIP was mono- and poly-ubiquitinated in MPM samples (Figure 1a), we searched which mechanisms are involved in LIP degradation. Compared to HMC, MPM cells displayed increased proteasome (Figure 5a), autophagy (Figure 5b) and lysosome activity (Figure 5c). Treatment of MPM cells with the proteasome inhibitor carfilzomib and the lysosome inhibitor chloroquine lowered the proteasome and lysosome activity of MPM to values comparable to HMC (Supplementary Figure 5a-c). Either carfilzomib or chloroquine prevented LIP degradation and activated the downstream effectors CHOP, TRB3 and caspase 3 (Figure 5d). Chloroquine is an inhibitor of autophagy and lysosomes [25, 26] (Supplementary Figure 5b-c). To better understand if both mechanisms are equally involved in LIP degradation, we used the autophagy inhibitor 3-methyladenine, which does not affect lysosome activity [25] (Supplementary Figure 5b-c). 3-methyladenine prevented LIP degradation and activated the CHOP/TRB3/caspase 3 axis (Supplementary Figure 6) at a lesser extent than chloroquine (Figure 5d), suggesting that autophagy likely plays an ancillary role in the removal of LIP.

The combination of carfilzomib and chloroquine was even more effective than each agent alone in activating the LIP/CHOP/TRB3/caspase 3 pathway (Figure 5d). The treatment with carfilzomib and chloroquine, alone or in combination, increased the accumulation of ubiquitinated LIP compared to untreated cells (Supplementary Figure 7a; Supplementary Table 4c). The same increase in ubiquitinated LIP was detected in cells treated with the triple combination carfilzomib + chloroquine + cisplatin. The ratio between ubiquitinated LIP/total LIP was lowered in carfilzomib-

and chloroquine-treated cells, in particular in the combination treatments carfilzomib + chloroquine or carfilzomib + chloroquine + cisplatin (Supplementary Figure 7b).

Carfilzomib and chloroquine combination was also the most effective in inducing ICD-related parameters (Supplementary Figure 8a-e). The immunologic effects of carfilzomib and chloroquine were likely due to the attenuated degradation of LIP, as demonstrated by the absence of calreticulin up-regulation in MPM cells lacking LIP (Supplementary Figure 8f). The triple combination of cisplatin with carfilzomib and chloroquine further activated LIP/CHOP/TRIB3/caspase 3 pathway and ICD (Figure 5d, Supplementary Figure 6a-e).

### 3.6.Combination of carfilzomib, chloroquine and cisplatin abrogates mesothelioma growth

Combined treatment of carfilzomib and chloroquine greatly reduced MPM cell proliferation (Figure 6a-b) and tumor growth *in vivo* (Figure 6c), in particular if associated with cisplatin. This triple combination significantly increased the number of CHOP- and caspase 3-positive intratumor cells (Figure 6d), and raised an anti-tumor immune response *in vivo*, as demonstrated by the increased tumor-infiltrating DC and $CD8^+$ T-lymphocytes (Figure 6e-f), and by the increased production of IFN-γ in the draining lymph nodes (Figure 6g). Neither significant alterations in hemocromocytometric parameters nor signs of liver, kidney, heart and muscle toxicity were detectable in animals treated with this regimen (Supplementary Table 6).

## 4. Discussion

Aim of this study was to investigate the possible role of LIP as effector of resistance to cisplatin, predictive factor of patient response to cisplatin, and possible target to improve the sensitivity to this drug in MPM.

Using cells isolated from MPM patients treated with cisplatin but characterized by low response to the drug (mean survival after the beginning of therapy: 13.11 months), we noticed that they had lower amount of LIP compared to HMC cells and higher rate of LIP ubiquitination. Ubiquitination of LIP is a typical sign of its degradation *via* proteasome and/or lysosome [18, 20, 27]. This is consistent with the observation that in all MPM cells when ubiquitination of LIP was higher, the

protein was lower in comparison with HMC that had lower LIP ubiquitination and higher LIP protein level. The rate of LIP ubiquitination strongly correlated with the *in vitro* resistance to cisplatin, measured as $IC_{50}$ of the drug: indeed, higher was LIP ubiquitination (i.e. lower LIP protein was), higher was $IC_{50}$ of cisplatin. Hence, we concluded that LIP loss due to its ubiquitination was related to resistance to cisplatin *in vitro*. We considered the PFS, defined as the survival with stable disease from the beginning of cisplatin therapy, and the OS of each patient, defined as the time passed from the starting of cisplatin therapy to the date of patient death. Patients with LIP ubiquitination higher or equal to median value were included in the so-called "LIP low" group, since the patient-derived cell line had very low/undetectable LIP protein. Patients with LIP ubiquitination lower or equal to median value were included in the so-called "LIP high" group, since the patient-derived cell line had higher LIP protein. "High LIP ubiquitination/LIP low" patients had the shortest PFS and OS, patients with "low LIP ubiquitination/LIP high" patients displayed the most prolonged PFS and OS after cisplatin treatment.

Although the small number of patients and the absence of a control group receiving different treatments makes difficult to separate the prognostic and the predictive role of LIP ubiquitination, our work provides the rationale to measure LIP ubiquitination in larger series of MPM tumors, in order the evaluate if this parameter - beside being a good indicator of the sensitivity to cisplatin *in vitro* - may be also predictive of the clinical response to cisplatin.

In chemoresistant tumor cells, the loss of LIP upregulates the expression of the drug efflux transporter P-glycoprotein [20], increasing the resistance of such cells to a broad spectrum of chemotherapeutic drugs. Platinum-derived agents, however, are not substrates of P-glycoprotein [28]. Therefore, the restoration of drug sensitivity by LIP, after its genetic over-expression or pharmacological inhibition of its degradation, must rely on a different mechanism.

Cisplatin triggers ER stress-dependent apoptosis [11], but MPM cells were refractory to these events. Our findings in primary MPM samples and MPM preclinical models suggests that cisplatin induces apoptosis via the ER-dependent CHOP/TRB3/caspase 3 axis only in the presence of LIP,

while LIP loss abrogated the cell death due to cisplatin-triggered ER stress. In cisplatin-treated cells, the ratio between ubiquitinated LIP/total LIP was unchanged compared to untreated cells: the continuous ubiquitination of LIP likely explains the absence of any pro-apoptotic effect induced by the drug in MPM cells. By contrast, the ubiquitinated LIP/total LIP ratio was decreased in LIP-transduced cells, suggesting that the excess of exogenous LIP may saturate the maximal ubiquitination capacity of MPM cells. In these conditions, a significant amount of LIP remained not-ubiquitinated and likely triggered the pro-apoptotic CHOP/TRB3/caspase 3 axis. This effect was particularly pronounced in cells treated with cisplatin that slightly increased the amount of endogenous LIP. The sum of endogenous LIP induced by cisplatin and exogenous LIP produced by the transfection with a LIP-overexpressing vector produced a huge increase in not-ubiquitinated LIP, allowing the induction of LIP-triggered dependent apoptosis.

However, our finding that LIP induction attenuated tumor growth in mice even without cisplatin indicates that LIP regulates additional mechanisms on top of ER stress.

One such mechanism involves the anti-tumor immune response. Indeed, inducible intra-tumor activation of LIP delayed tumor growth in immune-competent animals more than in immune-deficient mice, indicating that LIP attenuates MPM progression enhancing the anti-tumor immune response. Intriguingly, the combination cisplatin+LIP was even more effective than LIP induction. In tumor extracts, cisplatin produced a small activation of LIP, without however reducing tumor growth. Since ER stress often occurs in tumor bulk as a consequence of hypoxia or nutrient shortage [16] and these conditions are sufficient to induce LIP activation [17], it is likely that the ER stress exerted by the tumor environment and the low ER stress elicited by cisplatin produced the small induction of LIP. Such induction, however, was insufficient to trigger ER-dependent apoptosis, as demonstrated by the absent intratumor activation of CHOP and caspase 3. Previously, cisplatin was not thought to trigger anti-tumor immune response [22, 29]. However, a recent report revealed that in non-small cell lung cancer, cisplatin increased intratumor DC recruitment, tumor cell phagocytosis and expansion of anti-tumor $CD8^+$ T-lymphocytes [30]. Intratumor recruitment of

386 DC is mediated by cell surface expression of calreticulin [31]. ER stress (and thereby activation of
387 LIP) is necessary for triggering immune responses by cisplatin [32]. Our work demonstrates that
388 LIP induced calreticulin expression and the subsequent chain of immune responses, providing a
389 plausible mechanism by which LIP triggers an anti-tumor immune response and rescues the activity
390 of cisplatin via ER stress-dependent apoptosis and ICD.
391 Endogenous LIP is physiologically removed by proteasome and lysosomes [20]. Interestingly, a
392 high activity of proteasome and lysosome correlates with bad patient prognosis in MPM [33, 34].
393 The inhibition of one of these two degradation pathways may be compensated by the increase in the
394 other pathway, suggesting that only a simultaneous blockade of the two is required for restoring
395 LIP-triggered apoptosis in MPM cells. To achieve this goal, we employed the FDA-approved
396 proteasome inhibitor carfilzomib and the lysosome inhibitor chloroquine.
397 Bortezomib, another proteasome inhibitor, is known to induce apoptosis in MPM cells synergizing
398 with cisplatin and oxaliplatin if administered before platinum-based agents [33, 35]. Our work
399 provides the rationale for this observation, suggesting that this synergy may be reached only after
400 the bortezomib-induced accumulation of LIP, which, in turn, enhanced cisplatin cytotoxicity.
401 Also chloroquine induces apoptosis of MPM cells if associated with nutritional stress [36] or
402 PI3K/mTOR inhibition [20], two conditions that induce ER stress [15, 16, 37], suggesting that at
403 least part of the pro-apoptotic effect of chloroquine is triggered by ER dysfunctions. Since
404 carfilzomib and chloroquine act downstream the ubiquitination system and prevent the degradation
405 of ubiquitinated proteins by proteasome and lysosomes [24], these drugs may produce an “action
406 mass”-like effect: by blocking the degradation of ubiquitinated LIP *via* proteasome and lysosomes,
407 carfilzomib and chloroquine increased the amount of ubiquitinated LIP to a level saturating the
408 ubiquitination capacity of MPM cells. This saturation ultimately resulted in the accumulation of
409 not-ubiquitinated LIP that triggered the CHOP/TRIB3/caspase 3 pro-apoptotic pathway.
410 In addition to ER stress-linked pro-apoptotic mechanisms, carfilzomib and chloroquine are known
411 ICD inducers [12, 38].

Until now, synergistic anti-tumor effects exerted by combining proteasome and lysosome inhibitors with platinum derivatives [33, 35, 39] were reported only *in vitro*. Our study is the first one demonstrating that the combination treatment of carfilzomib, chloroquine and cisplatin is effective in preclinical models of cisplatin-resistant MPM, by inducing ER stress-dependent apoptosis and activating the host immune system against MPM. Such triple combination did not elicit detectable signs of systemic toxicity *in vivo*. Moreover, each agent used in our preclinical model has well-known pharmacodynamic, pharmacokinetic and toxicological profiles for the extensive clinical use. These considerations are encouraging in the perspective of translating the triple combination cisplatin, carfilzomib and chloroquine to clinical settings.

## Conclusions

Our work demonstrates that LIP levels strongly correlated with MPM response to cisplatin *in vitro*, providing the preliminary data to evaluate if the correlation between high LIP ubiquitination and low survival is valid in larger patients cohort. If the data reported in this study was confirmed, LIP ubiquitination may represent a factor predictive of clinical response to cisplatin. We suggest to include pharmacological inhibitors of LIP degradation, such as a combination of proteasome and lysosome inhibitors, in the number of strategies under evaluation to improve the response of MPM to the current treatment.

## Data availability

All data generated or analysed during this study are included in this published article and its supplementary information files.

## Conflict of interests

None.

## Funding

This work was supported by Italian Association for Cancer Research (IG15232 to CR), Italian Ministry of University and Research (EX60% Funding 2015 to SN and CR); Italian Ministry of Health (to LR and GVS); De Benedetti-Cherasco Foundation (Torino-Weizmann Collaborative Program: Scientific Cooperation and Exchange to MR and CR); Fondazione Cassa di Risparmio di Torino (to CR). ICS is recipient of PhD scholarships from the Italian Institute for Social Security (INPS). VM is a PhD fellow of Erasmus Mundus-ERAWEB Action 2 program.

The funding institutions had no role in the study design, data collection and analysis, or in writing the manuscript.

## References

[1] S. Remon, N. Reguart, J. Corral, P. Lianes, Malignant pleural mesothelioma: new hope in the horizon with novel therapeutic strategies. Cancer Treat. Rev. 41 (2015) 27-34.

[2] M.A. Bonelli, C. Fumarola, S. La Monica, R. Alfieri, New therapeutic strategies for malignant pleural mesothelioma. Biochem. Pharmacol. 123 (2017) 8-18.

[3] V. Izzi, L. Masuelli, I. Tresoldi, C. Foti, A. Modesti, R. Bei, Immunity and malignant mesothelioma: from mesothelial cell damage to tumor development and immune response-based therapies. Cancer Lett. 322 (2012) 18-34.

[4] L.A. Lievense, K. Bezemer, R. Cornelissen, M.E. Kaijen-Lambers, J.P. Hegmans, J.G. Aerts, Precision immunotherapy; dynamics in the cellular profile of pleural effusions in malignant mesothelioma patients. Lung Cancer 107 (2017) 36-40.

[5] S. Khanna, A. Thomas, D. Abate-Daga, J. Zhang, B. Morrow, S.M. Steinberg, et al., Malignant Mesothelioma Effusions Are Infiltrated by CD3(+) T Cells Highly Expressing PD-L1 and the PD-L1(+) Tumor Cells within These Effusions Are Susceptible to ADCC by the Anti-PD-L1 Antibody Avelumab. J. Thorac. Oncol. 11 (2016) 1993-2005.

[6] M.M. Awad, R.E. Jones, H. Liu, P.H. Lizotte, E.V. Ivanova, M. Kulkarni, et al., Cytotoxic T Cells in PD-L1-Positive Malignant Pleural Mesotheliomas Are Counterbalanced by Distinct Immunosuppressive Factors. Cancer Immunol. Res. 4 (2016) 1038-1048.

[7] J.G. Aerts, L.A. Lievense, H.C. Hoogsteden, J.P Hegmans, Immunotherapy prospects in the treatment of lung cancer and mesothelioma. Transl. Lung Cancer Res. 3 (2014) 34-45.

[8] R.A. Stahel, W. Weder, E. Felley-Bosco, U. Petrausch, A. Curioni-Fontecedro, I. Schmitt-Opitz, et al., Searching for targets for the systemic therapy of mesothelioma. Ann. Oncol. 26 (2015) 1649-1660.

[9] D.A. Fennell, Y. Summers, J. Cadranel, T. Benepal, D.C. Christoph, R. Lal, et al., Cisplatin in the modern era: The backbone of first-line chemotherapy for non-small cell lung cancer. Cancer Treat. Rev. 44 (2016) 42-50.

[10] S.E. Farber-Katz, H.C. Dippold, M.D. Buschman, M.C. Peterman, M. Xing, C.J. Noakes, et al., DNA damage triggers Golgi dispersal via DNA-PK and GOLPH3. Cell. 2014;156: 413-427.

[11] A. Mandic, J. Hansson, S. Linder, M. Shoshan, Cisplatin induces endoplasmic reticulum stress and nucleus-independent apoptotic signaling. J. Biol. Chem. 278 (2003) 278 9100-9106.

[12] L. Galluzzi, A. Buqué, O. Kepp, L. Zitvogel, G. Kroemer, Immunogenic cell death in cancer and infectious disease. Nat. Rev. Immunol. 7 (2017) 97-111.

[13] C. Riganti, B. Castella, J. Kopecka, I. Campia, M. Coscia, G. Pescarmona, et al., Zoledronic acid restores doxorubicin chemosensitivity and immunogenic cell death in multidrug-resistant human cancer cells. PLoS One. 8 (2013) e60975.

[14] C. Riganti, M.F. Lingua, I.C. Salaroglio, C. Falcomatà, L. Righi, D. Morena, et al., Bromodomain inhibition exerts its therapeutic potential in malignant pleural mesothelioma by promoting immunogenic cell death and changing the tumor immune-environment. Oncoimmunology. 7 (2017) e1398874.

[15] I. Kim, W. Xu, J. Reed, Cell death and endoplasmic reticulum stress: Disease relevance and therapeutic opportunities. Nat. Rev. Drug Discov. 7 (2008) 1013-1030.

488 [16] E. Chevet, C. Hetz, A. Samali, Endoplasmic reticulum stress-activated cell reprogramming in
489 oncogenesis. Cancer Discov. 5 (2015) 586-597.
490 [17] O. Meir, E. Dvash, A. Werman, M. Rubinstein, C/ebp-beta regulates endoplasmic reticulum
491 stress-triggered cell death in mouse and human models. PLoS One. 5 (2010) e9516.
492 [18] C. Chiribau, F. Gaccioli, C. Huang, C. Yuan, M. Hatzoglou, Molecular symbiosis of chop and
493 c/ebp beta isoform lip contributes to endoplasmic reticulum stress-induced apoptosis. Mol. Cell.
494 Biol. 30 (2010) 3722-3731.
495 [19] N. Ohoka, S. Yoshii, T. Hattori, K. Onozaki, H. Hayashi, Trb3, a novel er stress-inducible gene,
496 is induced via atf4-chop pathway and is involved in cell death. EMBO J. 24 (2005) 1243-1255.
497 [20] C. Riganti, J. Kopecka, E. Panada, S. Barak, M. Rubinstein, The role of C/EBP-β LIP in
498 multidrug resistance. J. Natl. Cancer Inst. 107 (2015) piidjv046.

499 [21] S. Doublier, D.C. Belisario, M. Polimeni, L. Annaratone, C. Riganti, E. Allia, et al., HIF-1
500 activation induces doxorubicin resistance in MCF7 3-D spheroids via P-glycoprotein expression: a
501 potential model of the chemo-resistance of invasive micropapillary carcinoma of the breast. BMC
502 Cancer. 12 (2012) e4.
503 [22] M. Obeid, A. Tesniere, F. Ghiringhelli, G.M. Fimia, L. Apetoh, J.L. Perfettini, et al.,
504 Calreticulin exposure dictates the immunogenicity of cancer cell death. Nat. Med. 13 (2007) 54-61
505 [23] J. Zhou, S-H. Tan, V. Nicolas, C. Bauvy, N-D. Yang, J. Zhang, et al., Activation of lysosomal
506 function in the course of autophagy via mTORC1 suppression and autophagosome-lysosome
507 fusion. Cell Res. 23 (2013) 508-523.
508 [24] I. Dikic, Proteasomal and Autophagic Degradation Systems. Annu. Rev. Biochem. 86 (2017)
509 193-224.
510 [25] Y-T. Wu, H-L. Tan, G. Shui, C. Bauvy, Q. Huang, M.R. Wenk, et al., Dual Role of 3-
511 Methyladenine in Modulation of Autophagy via Different Temporal Patterns of Inhibition on Class
512 I and III Phosphoinositide 3-Kinase. J. Biol. Chem. 285 (2010) 10850-10861.

513 [26] N. Echeverry, G. Ziltener, D. Barbone, W. Weder, R.A. Stahel, V.C. Broaddus, et al.,
514 Inhibition of autophagy sensitizes malignant pleural mesothelioma cells to dual PI3K/mTOR
515 inhibitors. Cell Death Dis. 6 (2015) e1757.
516 [27] Y. Li, E. Bevilacqua, C.B. Chiribau, M. Majumder, C. Wang, C.M Croniger, et al., Differential
517 control of the ccaat/enhancer-binding protein beta (c/ebp beta) products liver-enriched transcriptional
518 activating protein (lap) and liver- enriched transcriptional inhibitory protein (lip) and the regulation
519 of gene expression during the response to endoplasmic reticulum stress. J. Biol. Chem. 283 (2008)
520 22443-22456.
521 [28] M.M. Gottesman, T. Fojo, S.E. Bates, Multidrug resistance in cancer: role of ATP-dependent
522 transporters. Nat. Rev. Cancer. 2 (2002) 48-58.
523 [29] A. Tesniere, F. Schlemmer, V. Boige, O. Kepp, I. Martins, F. Ghiringhelli, et al., Immunogenic
524 death of colon cancer cells treated with oxaliplatin. Oncogene. 29 (2010) 482-491.
525 [30] E. Beyranvand Nejad, T.C. van der Sluis, S. van Duikeren, H. Yagita, G.M. Janssen, P.A. van
526 Veelen, et al., Tumor Eradication by Cisplatin Is Sustained by CD80/86-Mediated Costimulation of
527 CD8+ T Cells. Cancer Res. 76 (2016) 6017-6029.
528 [31] S. Di Blasio, I.M. Wortel, D.A. van Bladel, L.E. de Vries, T. Duiveman-de Boer, K. Worah, et
529 al., Human CD1c(+) DCs are critical cellular mediators of immune responses induced by
530 immunogenic cell death. Oncoimmunology. 5 (2016) e1192739.
531 [32] I. Martins, O. Kepp, F. Schlemmer, S. Adjemian, M. Tailler, S. Shen, et al., Restoration of the
532 immunogenicity of cisplatin-induced cancer cell death by endoplasmic reticulum stress. Oncogene.
533 30 (2011) 1147-1158.
534 [33] A.C. Borczuk, C.G.A. Cappellini, H.K. Kim, M. Hesdorffer, R.N. Taub, C.A. Powell,
535 Molecular profiling of malignant peritoneal mesothelioma identifies the ubiquitin–proteasome
536 pathway as a therapeutic target in poor prognosis tumors. Oncogene. 26 (2007) 610-617.

[34] C. Follo, C. Barbone, W.G. Richards, R. Bueno, V.C. Broaddus, Autophagy initiation correlates with the autophagic flux in 3D models of mesothelioma and with patient outcome. Autophagy. 12 (2016) 1180-1194.

[35] G.J. Gordon, M. Mani, G. Maulik, L. Mukhopadhyay, B.Y. Yeap, H.L. Kindler, et al., Preclinical studies of the proteasome inhibitor bortezomib in malignant pleural mesothelioma. Cancer Chemother. Pharmacol.61 (2008) 549-558.

[36] S. Battisti, D. Valente, L. Albonici, R. Bei, A. Modesti, C. Palumbo, Nutritional Stress and Arginine Auxotrophy Confer High Sensitivity to Chloroquine Toxicity in Mesothelioma Cells. Am. J. Respir. Cell. Mol. Biol. 46 (2012) 498-506.

[37] C. Appenzeller-Herzog, M.N. Hall, Bidirectional crosstalk between endoplasmic reticulum stress and mTOR signaling. Trends Cell. Biol. 22 (2012) 274-282.

[38] A.M. Dudek, A.D. Garg, D.V. Krysko, D. De Ruysscher, P. Agostinis, Inducers of immunogenic cancer cell death. Cytokine Growth Factor Rev. 24 (2013) 319-333.

[39] Y-J. Lee, G.J. Lee, S.S. Yi, S-H. Heo, C-R. Park, H-S. Nam, et al., Cisplatin and resveratrol induce apoptosis and autophagy following oxidative stress in malignant mesothelioma cells. Food Chem. Toxicol. 97 (2016) 96-107.

**Figure legends**

**Figure 1. Ubiquitination of LIP correlates with cisplatin resistance in mesothelioma**

**a.** Levels of *C/EBPβ* mRNA as determined by qRT-PCR in triplicates, in 3 primary human non-transformed mesothelial cells (HMC) and 9 primary human malignant pleural mesothelioma (MPM) samples. Epi: epithelioid; Bip: biphasic; Sar: sarcomatous. **b.** Expression and ubiquitination of C/EBP-β LAP and LIP in HMC and MPM samples. Whole cell lysate was immunoprecipitated (IP) with anti C/EBP-β antibody that recognize the common C-terminus C/EBP-β - i.e. either LIP or LAP - and the blot was probed (IB) with the anti C/EBP-β antibody, to detect total levels of C/EBP-β LAP and LIP isoforms, or with an anti-mono/poly-ubiquitin antibody, to detect the corresponding

ubiquitinated forms. *Upper-middle panels, last lane*: control immunoblot of MPM1 cell extract immunoprecipitated in the absence of antibody. Arrow, *middle panel*: ubiquitinated LIP, according to the expected molecular weight. Before immunoprecipitation, an aliquot of cell lysate was probed with an anti-β-tubulin antibody, to check that equal amounts of proteins from each extract were loaded in immunoprecipitation. The figure is representative of 1 out of 3 experiments. **c.** The mean band density of ubiquitinated LIP (indicated by the arrow, *middle panel*, Figure 1b) and the mean band density of total LIP (*upper panel*, Figure 1b) was calculated with the ImageJ software and expressed as arbitrary optical density units, setting the mean ratio between ubiquitinated LIP/total LIP in HMC to 1. Data are presented as means±SD (n=3). MPM vs HMC cells: *p<0.001. **d.** Correlation between $IC_{50}$ of cisplatin (Pt; Supplementary Table 3) and LIP ubiquitination, calculated with the ImageJ software . The mean band density of ubiquitinated LIP (indicated by the arrow, Figure 1b) was expressed as arbitrary optical density units, setting the mean band density in HMC samples to 1 (Supplementary Table 4a). **e-f.** LIP ubiquitination (indicated by the arrow, Figure 1b) was ranked according to mean band density of each patient (Supplementary Table 4a), and median value was calculated. Patients were classified as "LIP low" if LIP ubiquitination was higher or equal to the median value (n=5, i.e. patient 3, 4, 7,8, 9), "LIP high" if LIP ubiquitination was lower or equal to the median value (n=4, i.e. patient 1, 2, 5, 6). Progression free survival (panel **e**) and overall survival (panel **f**) probability was calculated using the Kaplan-Meier method. LIP high vs. LIP low group:*p<0.03 (panel **e**); *p<0.01 (panel **f**). UQ-LIP: ubiquitinated LIP

**Figure 2. LIP reconstitution induces apoptosis and rescues cisplatin-cytotoxicity in mesothelioma**

**a.** Immunoblot of the indicated proteins in extracts of MPM1 (epithelioid MPM) and MPM7 (sarcomatous MPM) cells, stably transfected with the doxycycline-inducible LIP-expression vector, cultured in the absence (-, Ctrl) or presence (+) of cisplatin (Pt, 25 μM) and doxycycline for 24 h. The figure is representative of 1 out of 3 experiments. **b**. Cell cycle analysis of cells treated as in **a**, performed by flow cytometry in duplicates. Pooled data of MPM 1-9 as means±SD (n=3). LIP-

589 treated vs. Ctrl cells:*p<0.01; LIP+Pt-treated cells vs. Pt-treated cells:°p<0.001. **c.** Cell proliferation
590 in cultures treated 8 h after seeding (time "0" in the graph) as in **a**. Pooled data of MPM 1-9 as
591 means±SD (n=4). LIP-treated vs. Ctrl cells (72-96 h):*p<0.01; LIP+Pt-treated cells vs. Pt-treated
592 cells (72-96 h):°p<0.001. **d**. Representative photographs of cells stained with crystal violet (96 h;
593 *left panel*) and quantitation of crystal violet-stained cells, expressed as percentage of viable cells
594 compared to untreated cells (*right panel*). Data of MPM1 and MPM7 cells are presented as
595 means±SD (n=4). Pt-treated vs. Ctrl cells:$^{\#}$p<0.05; LIP-treated vs. Ctrl cells:*p<0.001; LIP/LIP+Pt-
596 treated cells vs. Pt-treated cells:°p<0.001.

597 **Figure 3. LIP restoration primes mesothelioma cells for immunogenic cell death**

598 **a.** Immunoblot of C/EBPβ LAP and LIP in whole cell lysates of MPM1 and MPM7 cells,
599 transfected with the inducible expression vector for LAP (*left panel*) or LIP *(right pane*), cultured in
600 the absence (-, Ctrl) or presence (+) of doxycycline (Doxy). The figure is representative of 1 out of
601 3 experiments. **b**. ChIP showing the binding of LAP or LIP to the calreticulin (*CRT*) promoter (site
602 831-843). Bl: blank; DNA input: genomic DNA. The figure is a representative of 1 out of 3
603 experiments. **c.** Levels of calreticulin (*CRT*) mRNA as determined by qRT-PCR in triplicates.
604 Pooled data of MPM 1-9 as means±SD (n=3). LIP-expressing cells vs. un-induced cells:*p<0.001.
605 **d.** Surface calreticulin (CRT) as detected by flow cytometry in duplicates. The histograms represent
606 the results obtained on MPM1 and MPM7. **e**. Phagocytic index of MPM cells phagocytized by DC,
607 as determined by flow cytometry. Pooled data of MPM 1-9 as means±SD (n=3). LIP-expressing
608 cells vs. un-induced cells:*p<0.001. **f.** Percentage of $CD8^{+}CD107^{+}$T-lymphocytes as determined by
609 flow cytometry in duplicates. Pooled data of MPM 1-9 as means±SD (n=3). LIP-expressing cells
610 vs. un-induced cells:*p<0.001. **g.** IFN-γ levels in the supernatant of $CD8^{+}CD107^{+}$T-cells, measured
611 in duplicates. Pooled data of MPM 1-9 as means±SD (n=3). LIP-expressing cells vs. un-induced
612 cells:*p< 0.001.

613 **Figure 4. LIP overcomes cisplatin-resistance and immune-resistance *in vivo***

**a.** $1\times10^7$ AB1 inducibly expressing LIP (clone 1, Supplemnetary Figure 3) were injeted s.c. in 6-weeks-old female immune-competent or immune-deficient (nude) balb/C mice. When tumor reached the volume of 50 $mm^3$, animals (n=10/group) were randomized and treated on days 1,7 and 14 as follows: 1) control (Ctrl) group, treated with 0.1 ml saline solution intravenously (i.v.); 2) LIP group, treated with 1 mg/ml doxycycline in the drinking water to induce the LIP intratumorally; 3) cisplatin (Pt) group, treated with 5 mg/kg cisplatin i.v.; 4) LIP+cisplatin (LIP+Pt) group, treated with cisplatin and doxycycline to induce LIP. Data are means±SD. Pt/LIP+Pt groups vs. Ctrl group (days 15-21:immune-competent mice, day 21:immune-deficient/nude mice):*$p<0.001$; LIP+Pt group vs. Pt group (days 9-21:immune-competent and immune-deficient/nude mice):°$p<0.001$; LIP+Pt group vs. LIP group (days 9-21: immune-competent and immune-deficient/nude mice):$^{\#}p<0.005$; LIP+Pt group in immunocompetent vs. immune-deficient/nude mice: $p<0.005$ (not shown). **b**. Immunoblotting of C/EBPβ LAP and LIP from tumor extracts, to check LIP induction in mice treated with doxycycline. The figure is representative of extracts from two immune-deficient mice and two immune-competent mice. β-tubulin was used as control of equal protein loading. **c.** Sections of tumors from each group of immune-competent animals, stained with hematoxylin and eosin (HE; 20X objective; bar=100 µm), or immunostained with the indicated antibodies (63X objective; bar=10 µm). The photographs are representative of sections from 5 tumors/group. Data are means±SD. Pt/LIP+Pt groups vs. Ctrl group:*$p<0.005$; LIP+Pt group vs. Pt group:°$p<0.001$; LIP+Pt group vs. LIP group:$^{\#}p<0.05$. **d.** Percent of DC cells in tumors grown in immune-competent mice, treated by Pt, doxycycline (LIP) or their combination. The percent of DC was determined in duplicates by flow cytometry of single cell suspensions. **e**. Percent of $CD3^+CD8^+$T-lymphocytes measured as in **d**. Data of panels **d** and **e** are means±SD. Pt/LIP+Pt groups vs. Ctrl group:*$p<0.001$; LIP+Pt group vs. Pt group:°$p<0.001$; LIP+Pt group vs. LIP group:$^{\#}p<0.02$. **f.** IFN-γ levels as measured in duplicates in the supernatant of tumor-draining lymph nodes of immune-competent mice. Data of are means±SD. Pt/LIP+Pt groups vs. Ctrl group:*$p<0.001$; LIP+Pt group vs. Pt group:°$p<0.001$; LIP+Pt group vs. LIP group:$^{\#}p<0.05$.

**Figure 5. LIP undergoes proteasomal and lysosomal degradation in mesothelioma cells**

**a.** Proteasome activity as analyzed in 3 primary HMC and 9 primary human MPM samples, determined in duplicates by a chemiluminescence-based assay. Data are means±SD (n=3). MPM vs. HMC:*p<0.001. **b.** Autophagy activity as measured spectrofluorimetrically in duplicates. Data are means±SD (n=3). MPM vs HMC: *p<0.001. **c.** Lysosome activity as measured in duplicates by a spectrophotometric assay. Data are means±SD (n=3). MPM vs HMC:*p<0.001. **d.** Immunoblot of the indicated proteins in extracts of MPM1 and MPM7 cells, grown for 24 h in the absence (-), or presence of the proteasome inhibitor carfilzomib (20 nM, Ca), the lysosome inhibitor chloroquine (10 μM, Cq), or their combination, with or without, cisplatin (Pt, 25 μM), added for additional 24 h. The effects induced by cisplatin alone are reported in Figure 2a. The figure is representative of 1 out of 3 experiments.

**Figure 6. Carfilzomib and chloroquine rescue cisplatin anti-tumor effects *in vitro* and *in vivo***

**a.** Growth curves of MPM cells, treated 8 h (time "0" in the graph) after seeding with fresh medium (Ctrl), or media containing carfilzomib (20 nM, Ca), chloroquine (10 μM, Cq), or their combination, without or with cisplatin (Pt, 25 μM). The effects induced by cisplatin alone are reported in Figure 2c. Pooled data of MPM 1-9 as means±SD (n=4). All drug-treated cells vs. Ctrl cells (72-96 h):*p<0.001; Ca+Cq+Pt cells vs. Ca+Cq cells (72-96 h):°p<0.001. **b**. Representative photographs of cells stained with crystal violet (96 h). **c.** AB1 cells were injected s.c. in 6-weeks-old growth in immune-competent balb/C mice (n=10/group). When tumor reached the volume of 50 $mm^3$, animals (n=10/group) were randomized and treated on days 1, 7 and 14 as follows: 1) control (Ctrl) group, treated with 0.1 ml saline solution intravenously (i.v.); 2) carfilzomib (Ca) group, treated with 5 mg/kg carfilzomib i.v.; 3) chloroquine (Cq), treated with 10 mg/kg chloroquine *per os*; 4) carfilzomib+chloroquine (Ca+Cq) group, treated with both drugs; 5) carfilzomib+chloroquine+cisplatin (Ca+Cq+Pt) group, treated with carfilzomib, chloroquine and 5 mg/kg cisplatin i.v. (24 h after carfilzomib+chloroquine). Data are means±SD. All drug-treated cells vs. Ctrl group:*p<0.001; Ca+Cq+Pt group vs. Ca+Cq group:°p<0.001. **d.** Sections of tumors from

each group, stained with hematoxylin and eosin (HE; 20X objective; bar=100 µm), or immunostained with the indicated antibodies (63X objective; bar=10 µm). The percentage of CHOP- and cleaved caspase 3-positive cells as determined by analyzing sections from 5 mice of each group (110-93 cells/field), using the Photoshop program. "Ctrl" group intensity was taken as 100%. Data are means±SD. Treated groups vs. Ctrl group:*$p<0.002$; Ca+Cq+Pt group vs. Ca+Cq group:°$p<0.01$. **e.** Percentage of infiltrating DC in tumors grown in mice that were treated as in **d**. **f.** Percentage of infiltrating $CD3^+CD8^+$T-lymphocytes in these tumors. Data in panels **e** and **f**, determined in duplicates, are means±SD. All drug-treated groups vs. Ctrl group:*$p< 0.001$; Ca+Cq+Pt group vs. Ca+Cq group:°$p< 0.02$. **g.** IFN-γ levels in the supernatants of tumor-draining lymph nodes. Data determined in duplicates are means±SD. All drug-treated groups vs. Ctrl group: *$p<0.001$; Ca+Cq+Pt group vs. Ca+Cq group:°$p<0.05$.

# Loss of C/EBP-β LIP drives cisplatin resistance in malignant pleural mesothelioma

Joanna Kopecka[a,*], Iris C. Salaroglio[a,*], Luisella Righi[b], Roberta Libener[c], Sara Orecchia[c], Federica Grosso[d], Vladan Milosevic[a], Preeta Ananthanarayanan[a], Luisa Ricci[a], Enrica Capelletto[e], Monica Pradotto[e], Francesca Napoli[b], Massimo Di Maio[f], Silvia Novello[e], Menachem Rubinstein[g], Giorgio V. Scagliotti[e,*] , Chiara Riganti[a,*]

[a] Department of Oncology, University of Torino, via Santena 5/bis, 10126, Torino, Italy

[b] Pathology Unit, Department of Oncology at San Luigi Hospital, University of Torino, Regione Gonzole 10, 10043, Orbassano, Italy

[c] Pathology Division, S. Antonio and Biagio Hospital, Spalto Marengo, 15121, Alessandria, Italy

[d] Oncology Division, S. Antonio and Biagio Hospital, Spalto Marengo, 15121, Alessandria, Italy

[e] Thoracic Unit and Medical Oncology Division, Department of Oncology at San Luigi Hospital, Regione Gonzole 10, University of Torino, Orbassano, Italy

[f] Medical Oncology Division, Department of Oncology at Mauriziano Hospital, Largo Filippo Turati 62, 10128, University of Torino, Italy

[g] Department of Molecular Genetics, The Weizmann Institute of Science, Herzl Street 234, 76100, Rehovot, Israel

***** These authors equally contributed to the work

**Authors email addresses:** JK: joanna.kopecka@unito.it; ICS: irischiara.salaroglio@unito.it; LR: luisella.righi@unito.it; RL: rlibener@ospedale.al.it; SO: sorecchia@ospedale.al.it; FG: fgrosso@ospedale.al.it; VM: vladan.milosevic@unito.it; PA: preeta.ananthanarayanan@unito.it; LRic: luisa.ricci@gmail.com; EC: enrica.capelletto@gmail.com; MP: monica.pradotto@unito.it; FN: francesca.napoli@unito.it; MDM: massimo.dimaio@unito.it; SN: silvia.novello@unito.it; MR:

menachem.rubinstein@weizmann.ac.il; GVS: giorgio.scagliotti@unito.it; CR: chiara.riganti@unito.it

**Corresponding author**: Dr. Chiara Riganti, Department of Oncology, University of Torino, via Santena 5/bis, 10126, Torino, Italy; phone: +390116705857; fax: +390116705845; email: chiara.riganti@unito.it

**Abstract**

**Objectives.** Cisplatin-based chemotherapy is moderately active in malignant pleural mesothelioma (MPM) due to intrinsic drug resistance and to low immunogenicity of MPM cells. CAAT/enhancer binding protein (C/EBP)-β LIP is a pro-apoptotic and chemosensitizing transcription factor activated in response to endoplasmic reticulum (ER) stress.

**Materials and methods**. We investigated if LIP levels can predict the clinical response to cisplatin and survival of MPM patients receiving cisplatin-based chemotherapy. We studied the LIP-dependent mechanisms determining cisplatin-resistance and we identified pharmacological approaches targeting LIP, able to restore cisplatin sensitiveness, in patient-derived MPM cells and animal models. Results were analyzed by a one-way analysis of variance test.

**Results.** We found that LIP was degraded by constitutive ubiquitination in primary MPM cells derived from patients poorly responsive to cisplatin. LIP ubiquitination was directly correlated with cisplatin chemosensitivity and was associated with patients' survival after chemotherapy. Overexpression of LIP restored cisplatin's pro-apoptotic effect by activating CHOP/TRB3/caspase 3 axis and up-regulating calreticulin, that triggers MPM cell phagocytosis by dendritic cells and expanded autologous anti-tumor $CD8^+CD107^+$T-cytotoxic lymphocytes. Proteasome inhibitor carfilzomib and lysosome inhibitor chloroquine prevented LIP degradation. The triple combination of carfilzomib, chloroquine and cisplatin increased ER stress-triggered

apoptosis and immunogenic cell death in patients' samples, and reduced tumor growth in cisplatin-resistant MPM preclinical models.

**Conclusion.** The loss of LIP mediates cisplatin resistance, rendering LIP a possible predictor of cisplatin response in MPM patients. The association of proteasome and lysosome inhibitors reverses cisplatin resistance by restoring LIP levels and may represent a new adjuvant strategy in MPM treatment.

**Highlights**

- C/EBP-β LIP loss correlates with poor response to cisplatin in mesothelioma patients
- C/EBP-β LIP loss is due to its constitutive ubiquitination and degradation
- Lack of C/EBP-β LIP prevents cisplatin-induced apoptosis and immunogenic cell death
- Proteasome and lysosome inhibitors restoring C/EBP-β LIP rescue cisplatin efficacy

**Keywords:** malignant pleural mesothelioma; CAAT/enhancer binding protein; cisplatin resistance; endoplasmic reticulum stress; immunogenic cell death

**Abbreviations:** ANOVA, analysis of variance; ATF6, activating transcription factor 6; C/EBP, CAAT/enhancer binding protein; IRE1, inositol-requiring enzyme 1; CHOP/GADD153; C/EBP homologous protein/growth arrest/DNA damage inducible 153; CEA, carcino-embrionic antigen; ChIP, chromatin immunoprecipitation; DC, dendritic cells; ER, endoplasmic reticulum; EMA, epithelial membrane antigen; EIF2AK3/PERK, eukaryotic translation initiation factor-2α kinase 3; FBS, fetal bovine serum; ICD, immunogenic cell death; HMC, human mesothelial cells; MPM, malignant pleural mesothelioma; OS: overall survival; qRT-PCR, quantitative Real Time-PCR; PFS: progression free survival; SPSS, Statistical Package for Social Science; TBS, Tris-buffered

saline; TRB3, *tribbles*-related protein 3; UPN, Unknown Patient Number; WT1, Wilms tumor-1 antigen

## 1. Introduction

Malignant pleural mesothelioma (MPM), an asbestos-related cancer, is usually diagnosed at advanced stage, when chemotherapy - based on cisplatin associated with pemetrexed or raltitrexed - is the only available therapeutic option. [1,2]. The success of chemotherapy is limited by the intrinsic chemoresistance [1] and immune-evasive nature of MPM. Such immune-evasive microenvironment in MPM relies on the presence of immune-suppressive/immune-tolerant cells in the MPM [3, 4], on the high levels of immune-suppressive immune-checkpoints on both MPM cells and surrounding T-lymphocytes [5, 6], on the low amount of tumor-associated antigens of MPM cells [7], due to its low mutational burden [8].

In sensitive cells, cisplatin induces DNA damage, hampers DNA repair [9] and elicits nuclear-independent effects, such as dispersal of Golgi apparatus [10] and apoptosis induced by endoplasmic reticulum (ER) stress [11]. Upon ER stress, cancer cells expose on their surface the "eat-me" signal calreticulin, leading to dendritic cells (DC)-mediated phagocytosis and activation of autologous anti-tumor cytotoxic $CD8^+$T-lymphocytes [12]. This process is known as immunogenic cell death (ICD) [12]. MPM cells however do not translocate calreticulin from ER to surface [13, 14], resulting ICD-refractory. This is an additional mechanism explaining the low immunogenicity of MPM cell.

Solid tumors respond to chemotherapy-induced ER stress by activating adaptation and survival pathways if the stress is limited, or pro-apoptotic pathways if the stress persists [15, 16]. The ER stress-induced transcription factor CAAT/enhancer binding protein (C/EBP)-β is involved in both responses. At the early ER stress phase, the pro-survival isoform C/EBP-β LAP is produced. Upon prolonged ER stress, the isoform C/EBP-β LIP (LIP) is formed and activates C/EBP homologous protein/growth arrest/DNA damage inducible 153 (CHOP/GADD153) protein, which promotes apoptosis by activating *tribbles*-related protein 3 (TRB3) and caspase 3 [17-20]. At the present there are no data available about gene alterations (mutation, amplification or deletion) in the 87 MPM evaluated by the Tissue Cancer Genome Atlas (https://cancergenome.nih.gov), nor about the

104 expression of C/EBP-β LAP/LIP isoforms in MPM, according to Protein Tissue Atlas
105 (http://www.proteinatlas.org).
106 We recently reported that chemoresistant tumors lack LIP, because of its constitutive ubiquitination.
107 LIP loss mediates chemoresistance by increasing the expression of the drug efflux transporter P-
108 glycoprotein and by preventing the ER stress-dependent pro-apoptotic response [12].
109 Here, we investigated if LIP mediates the resistance to cisplatin in MPM. We identified clinically
110 feasible pharmacological strategies that restore the sensitivity of MPM to cisplatin by preventing
111 LIP degradation.

112 **2. Materials and methods**

113 **2.1.Chemicals.** Cell culture plastic ware were obtained from Falcon (Becton Dickinson, Franklin
114 Lakes, NJ). Electrophoresis reagents were obtained from Bio-Rad Laboratories (Hercules, CA).
115 Carfilzomib was purchased from Biorbyt Ltd. (Cambridge, UK) and torin 1 was from Selleckchem
116 (Munich, Germany). The protease inhibitor cocktail set III was obtained from Millipore (Billerica,
117 MA). Unless specified otherwise, all reagents were purchased from Sigma Chemicals Co (St. Louis,
118 MO).
119 **2.1.Cells.** Primary human mesothelial cells (HMC) were isolated from three patients with pleural
120 fluid secondary to congestive heart failure, with no history of a malignant disease. Nine primary
121 human MPM samples (3 epithelioid MPM, 3 biphasic MPM, 3 sarcomatous MPM) were obtained
122 from diagnostic thoracoscopies. Histological and clinical features are shown in Supplementary
123 Tables 1-2. All patients, identified with Unknown Patient Numbers (UPN), received 5 cycles of
124 cisplatin 75 mg/m$^2$ every 21 days. Tissue was digested in medium containing 1 mg/ml collagenase
125 and 0.2 mg/ml hyaluronidase for 1 h at 37°C. Cells were seeded in culture and used within passage
126 6. The Ethical Committee of Biological Bank of Mesothelioma, S. Antonio e Biagio Hospital,
127 Alessandria, Italy, and San Luigi Gonzaga Hospital, Orbassano, Italy, approved the study
128 (#9/11/2011; #126/2016). Murine AB1 cells were purchased from Sigma Chemicals Co. Cells were

grown in Ham's F10 nutrient mixture medium (primary HMC/MPM cells) or DMEM (AB1 cells), supplemented with 10% v/v fetal bovine serum, 1% v/v penicillin-streptomycin.

**2.3.Quantitative Real Time-PCR (qRT-PCR).** RNA was extracted and reverse-transcribed using the iScript™ cDNA Synthesis Kit (Bio-Rad Laboratories). qRT-PCR was performed using IQ™ SYBR Green Supermix (Bio-Rad Laboratories). The same cDNA preparation was used for measuring genes of interest and the housekeeping gene *S14*. Primer sequences were designed using qPrimerDepot software (http://primerdepot.nci.nih.gov/). Relative gene expression levels were calculated using Gene Expression Quantitation software (Bio-Rad Laboratories).

**2.4.Immunoblotting.** Protein or tumor extracts (20 μg) were subjected to SDS-PAGE and probed with the following antibodies: C/EBP-β (directed against the common C-terminus of LIP and LAP, Santa Cruz Biotechnology Inc., Santa Cruz, CA), CHOP/GADD153 (Abcam, Cambridge, UK), TRB3 (Proteintech, Chicago, IL), caspase-3 (GeneTex, Hsinhu City, Taiwan), β-tubulin (Santa Cruz Biotechnology Inc.). To detect ubiquitinated C/EBP-β, 100 μg protein extracts were immuno-precipitated overnight with the anti-C/EBP-β antibody, using 25 μl of PureProteome Magnetic Beads (Millipore). Immunoprecipitated samples were then probed with an anti-mono/polyubiquitin antibody (Axxora). Blotting was followed by the peroxidase-conjugated secondary antibody. The membranes were washed with Tris-buffered saline/Tween 0.01% v/v and proteins were detected by enhanced chemiluminescence. Band density was calculated using ImageJ software (http://www.rsb.info.nih.gov/ij/).

**2.5.Cell viability and growth**. Cell viability with neutral red staining and crystal violet staining were performed as reported [20]. $IC_{50}$ was calculated with the CompuSyn software (http://www.combosyn.com). Quantitation of crystal violet staining was performed by dissolving crystal violet with 1% v/v acetic acid and reading the absorbance of each well at 570 nm (HT Synergy 96-well microplate reader, Bio-Tek Instruments, Winoosky, VT).The mean absorbance of

153 untreated cells was considered 100%; the absorbance units of the other experimental conditions
154 were expressed as percentage towards untreated cells.

155 **2.6.Cell cycle analysis.** $1\times10^4$ cells were harvested, washed with PBS, treated with 0.25 mg/ml
156 RNAse and stained for 15 min with 50 µg/ml propidium iodide. Cell cycle distribution was
157 analyzed by Guava® easyCyte flow cytometer (Millipore, Billerica, MA), using the InCyte
158 software (Millipore).
159 **2.7.Over-expression of C/EBP-β LAP and LIP.** The pcDNA4/TO expression vectors (Invitrogen
160 Life Technologies, Milan, Italy) for LAP and LIP, produced as reported previously [17], were co-
161 transduced with pcDNA6/TR vector (Invitrogen Life Technologies) in parental cells. Stable TetON
162 clones were generated by selecting cells with 2 µg/ml blasticidin S (Invitrogen Life Technologies)
163 and 100 µg/ml zeocin (InvivoGen, San Diego, CA). LAP and LIP induction was activated by
164 adding 1 µg/ml doxycycline in the culture medium.

165 **2.8.C/EBP-β LIP silencing.** $2\times10^6$ cells in 0.25 ml serum/antibiotic-free medium were transfected
166 either with non-targeting scrambled siRNA pools or siRNA pools specifically targeting LIP
167 sequence (customized ON-TARGETplus, Dharmacon RNAi Technologies; Dharmacon, Lafayette,
168 CO), employing DharmaFECT 1 reagent (Dharmacon), as per manufacturer's protocol.
169 **2.9.Chromatin immunoprecipitation (ChIP).** To determine the binding of LAP and LIP to
170 calreticulin promoter we performed ChIP as described [21], using the anti-C/EBP-β antibody
171 directed against the common C-terminus of LAP and LIP. Putative binding sites of C/EBP-β were
172 identified using the Gene Promoter Miner software (http://gpminer.mbc.nctu.edu.tw/). PCR primers
173 were designed using Primer3 software (http://primer3.ut.ee/).
174 **2.10.Calreticulin expression, phagocytosi and T-lymphocyte activation.** Surface calreticulin was
175 measured by flow cytometry as reported [22]. DC were generated from peripheral blood samples of
176 patients, collected before starting chemotherapy, as previously reported [13]. Phagocytosis assays
177 were performed as detailed in [22]. Active anti-tumor cytotoxic $CD8^+CD107^+$T-lymphocytes,

obtained from autologous T-lymphocytes (co-cultured 10 days with DC after phagocytosis) and isolated with the Pan T Cell Isolation Kit (Miltenyi Biotec., Bergisch Gladbach, Germany), were measured by flow cytometry [13]. The production of IFN-γ in the culture supernatant of $CD8^+$T-cells co-cultured with DC or in the supernatant of tumor-draining lymph nodes - a second parameter of $CD8^+$T-cells cytotoxic activity - was measured with the Human IFN-γ DuoSet Development Kit (R&D Systems, Minneapolis, MN).

**2.11.*In vivo* tumor growth.** $1\times10^7$ AB1 cells expressing LIP upon doxycycline administration in drinking water, mixed with 100 µl Matrigel, were injected subcutaneously (s.c.) in 6-weeks-old female immune-competent or immune-deficient (nude) balb/C mice (Charles River Laboratories Italia, Calco), housed (5 per cage) under 12 h light/dark cycle, with food and drinking provided *ad libitum*. Tumor growth was measured daily by caliper, according to the equation $(LxW^2)/2$, where L=tumor length and W=tumor width. When tumor reached the volume of 50 $mm^3$, animals were randomized and treated as reported in the Figure Legends. Tumor volumes were monitored by caliper and animals were euthanized at day 21 after randomization with zolazepam (0.2 ml/kg) and xylazine (16 mg/kg). The hemocromocytometric analyses were performed with a UniCel DxH 800 Coulter Cellular Analysis System (Beckman Coulter, Miami, FL) on blood collected immediately after sacrificing the mice. Hematochemical parameters were analyzed using the respective kits from Beckman Coulter Inc. Animal care and experimental procedures, according to EU Directive 2010/63, were approved by the Bio-Ethical Committee of the Italian Ministry of Health (#122/2015-PR).

**2.12.Immunohistochemistry and intratumor immune infiltrate analysis**. Tumors were resected and fixed in 4% v/v paraformaldehyde, stained with hematoxylin/eosin or immunostained for CHOP or cleaved(Asp175)-caspase 3 (Cell Signaling Technology Inc., Danvers, MA), followed by a peroxidase-conjugated secondary antibody. Nuclei were counter-stained with hematoxylin. Sections were examined with a Leica DC100 microscope. Excised tumors were digested with 1 mg/ml collagenase and 0.2 mg/ml hyaluronidase (1h at 37°C) and filtered using a 70 µm cell

strainer to obtain a single cell suspension. Infiltrating immune cells were collected by centrifugation on Ficoll-Hypaque density gradient and subjected to immune phenotyping by flow cytometry, using antibodies against CD11c for DC, CD3 and CD8 for T-lymphocytes (Miltenyi Biotec.). Draining lymph nodes were collected, homogenized for 30 s at 15 Hz, using a TissueLyser II device (Qiagen, Hilden, Germany) and centrifuged at 12000 x g for 5 minutes. The supernatant was used to measure the amount of IFN-γ.

**2.13.Proteasome, autophagy and lysosome activity.** Proteasome activity was measured with the Proteasome-Glo™ Cell-Based Assays (Promega Corporation). Autophagy activity was measured using the Autophagy Assay Kit (Sigma Chemicals Co.). The activity of cathepsin L, taken as an index of lysosome activity, was measured as reported [23].

**2.14.Statistical analysis.** All data in the text and figures are provided as means±SD. The results were analysed by a one-way analysis of variance (ANOVA), using Statistical Package for Social Science (SPSS) software (IBM SPSS Statistics v.19). $p<0.05$ was considered significant. Overall survival was defined as the time passed from the starting of cisplatin therapy to the date of death (all patients were dead at the time of analysis). The Kaplan-Meier method was used to calculate overall survival. Log rank test was used to compare the outcome of the two groups. The sample size was calculated with the G*Power software (www.gpower.hhu.de), setting $\alpha \leq 0.05$ and $1-\beta=0.80$.

## 3. Results

### 3.1.LIP is constitutively ubiquitinated in mesothelioma and correlates with cisplatin resistance

*C/EBP-β* mRNA was equally expressed in primary non-transformed HMC and MPM cells (Figure 1a). By contrast, C/EBP-β LAP protein was detected in both HMC and MPM samples, LIP was detectable only in HMC. The absence or very low expression of LIP in MPM was due to its higher ubiquitination: lower was the level of LIP in MPM (*upper panel*, Figure 1b), higher was LIP ubiquitination (*middle panel*, Figure 1b; Figure 1c), suggesting that LIP ubiquitination can be paralleled by its degradation, as it occurs for most ubiquitinated proteins [24] All MPM samples were significantly more resistant to cisplatin *in vitro* compared to HMC (Supplementary Table 3).

Ubiquitinated LIP was directly correlated with the $IC_{50}$ of cisplatin (Figure 1d). LIP ubiquitination was also significantly associated with patients' progression free survival (PFS; Figure 1e) and overall survival (OS; Figure 1f) after cisplatin therapy: median PFS was 2.2 months, median OS was 9 months (Supplementary Table 2) in the top 5 patients (UPN 3, 4, 7, 8, 9) with highest LIP ubiquitination (LIP ubiquitination higher or equal to median value, Supplementary Table 4a). This group was called "LIP low group" in Figure 1e-f, since patient-derived cell had lower levels of LIP protein (Figure 1b, *upper panel*). Median PFS and OS were 5.3 and 16 months respectively (Supplementary Table 2) in the top 4 patients (UPN 1, 2, 5, 6) with lowest LIP ubiquitination (LIP ubiquitination lower or equal to median value, Supplementary Table 4a). This group was defined as "LIP high group" in Figure 1e-f, since patient-derived cells had higher levels of LIP protein (Figure 1b, *upper panel*).

### 3.2.Reconstitution of LIP restores cisplatin-induced cell death by activating ER stress-mediated apoptosis

To investigate whether there was a causal relationship between the loss of LIP and the resistance to cisplatin, we induced overexpression of exogenous LIP in MPM cells (Figure 2a). LIP transduced cells were more sensitive to cisplatin (Supplementary Table 5), activated the pro-apoptotic CHOP/TRB3/caspase 3 axis (Figure 2a), increased the percentage of sub-G1 apoptotic cells, reduced the percentage of cells entering the S-phase (Figure 2b), decreased cell proliferation (Figure 2c-d).

Cisplatin did not activate the LIP/CHOP/TRB3/caspase 3 axis, neither affected cell cycle, nor proliferation, in non-transduced MPM cells, whereas LIP induction restored all these events. The combination "LIP induction+cisplatin treatment" was superior to LIP induction only (Figure 2a-d). Although cisplatin slightly increased LIP amount, it did not change the basal rate of LIP ubiquitination, meaning that the induced LIP was ubiquitinated (Supplementary Figure 1a; Supplementary Table 4b) and subsequently degraded by the cell. The ratio ubiquitinated LIP/total LIP, calculated by densitometric analysis, was unchanged compared to untreated cells

(Supplementary Figure 1b). Also, in LIP-transduced cells, LIP protein underwent ubiquitination (Supplementary Figure 1a; Supplementary Table 4b). However, the ratio ubiquitinated LIP/total LIP was decreased in this case (Supplementary Figure 1b).

### 3.3.LIP triggers immunogenic cell death in mesothelioma cells

As observed above, MPM cells are refractory to ICD mediated by calreticulin [13, 14]. Two predicted binding sites for C/EBP transcription factors are present in calreticulin promoter at position 831-843 and 1302-1313 (Supplementary Figure 2a). The former one contains a CCAAT box motif (Supplementary Figure 2b). To investigate whether C/EBP-β interacts with calreticulin promoter, we used MPM clones constitutively overexpressing LAP or LIP (Figure 3a). Of note, LIP bound the 831-843 site (Figure 3b). LIP-transduced cells increased calreticulin mRNA and surface protein (Figure 3c-d), were easily phagocytized by DC (Figure 3e), expanded autologous activated $CD8^+$ $CD107^+$ T-lymphocytes producing IFN-γ (Figures 3f-g). By contrast, LAP overexpressing cells did not differ from non-transduced MPM samples (Figure 3c-g).

As a proof of concept of the role of LIP in these process, we silenced the exogenously expressed LIP in MPM cells (Supplementary Figure 3a). In LIP-silenced cells calreticulin expression, phagocytosis and antitumor cytotoxic T-lymphocyte expansion were abrogated (Supplementary Figures 3b-d), demonstrating the critical role of LIP as calreticulin inducer and ICD effector in MPM.

### 3.4.LIP expression restores sensitivity to cisplatin and immune-mediated death *in vivo*

To validate the effects of LIP overexpression *in vivo*, we produced doxycycline-inducible LIP clones from AB1 cells (Supplementary Figure 4), a murine mesothelioma cell line syngeneic with balb/C mice. $IC_{50}$ of cisplatin was 91.08 ± 17.18 μM in un-induced AB1 cells, in line with the most cisplatin-resistant human MPM cells (Supplementary Table 3). Accordingly, AB1-tumors were unresponsive to cisplatin when implanted in mice (Figure 4a). Upon induction of LIP (Figure 4b), the tumor growth was reduced in both immune-deficient and immune-competent mice (Figure 4a) and showed increased percentage of tumor cells positive for CHOP and cleaved caspase 3 (Figure

3c), in particular in LIP-induced/cisplatin-treated mice. The antitumor effects of LIP + cisplatin were stronger in immune-competent mice, at least during the early development of MPM (Figure 4a), suggesting that immune system activation plays a significant role in delaying MPM growth. In immune-competent mice, LIP induction increased intratumor infiltrating DC and $CD8^+$ T-lymphocytes, and production of IFN-γ in draining lymph nodes (Figure 4d-f). Cisplatin enhanced all these events in LIP-expressing tumors (Figure 4d-f).

**3.5.LIP undergoes proteasomal and lysosomal degradation**

Since LIP was mono- and poly-ubiquitinated in MPM samples (Figure 1a), we searched which mechanisms are involved in LIP degradation. Compared to HMC, MPM cells displayed increased proteasome (Figure 5a), autophagy (Figure 5b) and lysosome activity (Figure 5c). Treatment of MPM cells with the proteasome inhibitor carfilzomib and the lysosome inhibitor chloroquine lowered the proteasome and lysosome activity of MPM to values comparable to HMC (Supplementary Figure 5a-c). Either carfilzomib or chloroquine prevented LIP degradation and activated the downstream effectors CHOP, TRB3 and caspase 3 (Figure 5d). Chloroquine is an inhibitor of autophagy and lysosomes [25, 26] (Supplementary Figure 5b-c). To better understand if both mechanisms are equally involved in LIP degradation, we used the autophagy inhibitor 3-methyladenine, which does not affect lysosome activity [25] (Supplementary Figure 5b-c). 3-methyladenine prevented LIP degradation and activated the CHOP/TRB3/caspase 3 axis (Supplementary Figure 6) at a lesser extent than chloroquine (Figure 5d), suggesting that autophagy likely plays an ancillary role in the removal of LIP.

The combination of carfilzomib and chloroquine was even more effective than each agent alone in activating the LIP/CHOP/TRB3/caspase 3 pathway (Figure 5d). The treatment with carfilzomib and chloroquine, alone or in combination, increased the accumulation of ubiquitinated LIP compared to untreated cells (Supplementary Figure 7a; Supplementary Table 4c). The same increase in ubiquitinated LIP was detected in cells treated with the triple combination carfilzomib + chloroquine + cisplatin. The ratio between ubiquitinated LIP/total LIP was lowered in carfilzomib-

and chloroquine-treated cells, in particular in the combination treatments carfilzomib + chloroquine or carfilzomib + chloroquine + cisplatin (Supplementary Figure 7b).

Carfilzomib and chloroquine combination was also the most effective in inducing ICD-related parameters (Supplementary Figure 8a-e). The immunologic effects of carfilzomib and chloroquine were likely due to the attenuated degradation of LIP, as demonstrated by the absence of calreticulin up-regulation in MPM cells lacking LIP (Supplementary Figure 8f). The triple combination of cisplatin with carfilzomib and chloroquine further activated LIP/CHOP/TRIB3/caspase 3 pathway and ICD (Figure 5d, Supplementary Figure 6a-e).

### 3.6.Combination of carfilzomib, chloroquine and cisplatin abrogates mesothelioma growth

Combined treatment of carfilzomib and chloroquine greatly reduced MPM cell proliferation (Figure 6a-b) and tumor growth *in vivo* (Figure 6c), in particular if associated with cisplatin. This triple combination significantly increased the number of CHOP- and caspase 3-positive intratumor cells (Figure 6d), and raised an anti-tumor immune response *in vivo*, as demonstrated by the increased tumor-infiltrating DC and $CD8^+$ T-lymphocytes (Figure 6e-f), and by the increased production of IFN-γ in the draining lymph nodes (Figure 6g). Neither significant alterations in hemocromocytometric parameters nor signs of liver, kidney, heart and muscle toxicity were detectable in animals treated with this regimen (Supplementary Table 6).

## 4. Discussion

Aim of this study was to investigate the possible role of LIP as effector of resistance to cisplatin, predictive factor of patient response to cisplatin, and possible target to improve the sensitivity to this drug in MPM.

Using cells isolated from MPM patients treated with cisplatin but characterized by low response to the drug (mean survival after the beginning of therapy: 13.11 months), we noticed that they had lower amount of LIP compared to HMC cells and higher rate of LIP ubiquitination. Ubiquitination of LIP is a typical sign of its degradation *via* proteasome and/or lysosome [18, 20, 27]. This is consistent with the observation that in all MPM cells when ubiquitination of LIP was higher, the

protein was lower in comparison with HMC that had lower LIP ubiquitination and higher LIP protein level. The rate of LIP ubiquitination strongly correlated with the *in vitro* resistance to cisplatin, measured as $IC_{50}$ of the drug: indeed, higher was LIP ubiquitination (i.e. lower LIP protein was), higher was $IC_{50}$ of cisplatin. Hence, we concluded that LIP loss due to its ubiquitination was related to resistance to cisplatin *in vitro*. We considered the PFS, defined as the survival with stable disease from the beginning of cisplatin therapy, and the OS of each patient, defined as the time passed from the starting of cisplatin therapy to the date of patient death. Patients with LIP ubiquitination higher or equal to median value were included in the so-called "LIP low" group, since the patient-derived cell line had very low/undetectable LIP protein. Patients with LIP ubiquitination lower or equal to median value were included in the so-called "LIP high" group, since the patient-derived cell line had higher LIP protein. "High LIP ubiquitination/LIP low" patients had the shortest PFS and OS, patients with "low LIP ubiquitination/LIP high" patients displayed the most prolonged PFS and OS after cisplatin treatment.

Although the small number of patients and the absence of a control group receiving different treatments makes difficult to separate the prognostic and the predictive role of LIP ubiquitination, our work provides the rationale to measure LIP ubiquitination in larger series of MPM tumors, in order the evaluate if this parameter - beside being a good indicator of the sensitivity to cisplatin *in vitro* - may be also predictive of the clinical response to cisplatin.

In chemoresistant tumor cells, the loss of LIP upregulates the expression of the drug efflux transporter P-glycoprotein [20], increasing the resistance of such cells to a broad spectrum of chemotherapeutic drugs. Platinum-derived agents, however, are not substrates of P-glycoprotein [28]. Therefore, the restoration of drug sensitivity by LIP, after its genetic over-expression or pharmacological inhibition of its degradation, must rely on a different mechanism.

Cisplatin triggers ER stress-dependent apoptosis [11], but MPM cells were refractory to these events. Our findings in primary MPM samples and MPM preclinical models suggests that cisplatin induces apoptosis via the ER-dependent CHOP/TRB3/caspase 3 axis only in the presence of LIP,

while LIP loss abrogated the cell death due to cisplatin-triggered ER stress. In cisplatin-treated cells, the ratio between ubiquitinated LIP/total LIP was unchanged compared to untreated cells: the continuous ubiquitination of LIP likely explains the absence of any pro-apoptotic effect induced by the drug in MPM cells. By contrast, the ubiquitinated LIP/total LIP ratio was decreased in LIP-transduced cells, suggesting that the excess of exogenous LIP may saturate the maximal ubiquitination capacity of MPM cells. In these conditions, a significant amount of LIP remained not-ubiquitinated and likely triggered the pro-apoptotic CHOP/TRB3/caspase 3 axis. This effect was particularly pronounced in cells treated with cisplatin that slightly increased the amount of endogenous LIP. The sum of endogenous LIP induced by cisplatin and exogenous LIP produced by the transfection with a LIP-overexpressing vector produced a huge increase in not-ubiquitinated LIP, allowing the induction of LIP-triggered dependent apoptosis.

However, our finding that LIP induction attenuated tumor growth in mice even without cisplatin indicates that LIP regulates additional mechanisms on top of ER stress.

One such mechanism involves the anti-tumor immune response. Indeed, inducible intra-tumor activation of LIP delayed tumor growth in immune-competent animals more than in immune-deficient mice, indicating that LIP attenuates MPM progression enhancing the anti-tumor immune response. Intriguingly, the combination cisplatin+LIP was even more effective than LIP induction. In tumor extracts, cisplatin produced a small activation of LIP, without however reducing tumor growth. Since ER stress often occurs in tumor bulk as a consequence of hypoxia or nutrient shortage [16] and these conditions are sufficient to induce LIP activation [17], it is likely that the ER stress exerted by the tumor environment and the low ER stress elicited by cisplatin produced the small induction of LIP. Such induction, however, was insufficient to trigger ER-dependent apoptosis, as demonstrated by the absent intratumor activation of CHOP and caspase 3. Previously, cisplatin was not thought to trigger anti-tumor immune response [22, 29]. However, a recent report revealed that in non-small cell lung cancer, cisplatin increased intratumor DC recruitment, tumor cell phagocytosis and expansion of anti-tumor $CD8^+$ T-lymphocytes [30]. Intratumor recruitment of

386 DC is mediated by cell surface expression of calreticulin [31]. ER stress (and thereby activation of
387 LIP) is necessary for triggering immune responses by cisplatin [32]. Our work demonstrates that
388 LIP induced calreticulin expression and the subsequent chain of immune responses, providing a
389 plausible mechanism by which LIP triggers an anti-tumor immune response and rescues the activity
390 of cisplatin via ER stress-dependent apoptosis and ICD.
391 Endogenous LIP is physiologically removed by proteasome and lysosomes [20]. Interestingly, a
392 high activity of proteasome and lysosome correlates with bad patient prognosis in MPM [33, 34].
393 The inhibition of one of these two degradation pathways may be compensated by the increase in the
394 other pathway, suggesting that only a simultaneous blockade of the two is required for restoring
395 LIP-triggered apoptosis in MPM cells. To achieve this goal, we employed the FDA-approved
396 proteasome inhibitor carfilzomib and the lysosome inhibitor chloroquine.
397 Bortezomib, another proteasome inhibitor, is known to induce apoptosis in MPM cells synergizing
398 with cisplatin and oxaliplatin if administered before platinum-based agents [33, 35]. Our work
399 provides the rationale for this observation, suggesting that this synergy may be reached only after
400 the bortezomib-induced accumulation of LIP, which, in turn, enhanced cisplatin cytotoxicity.
401 Also chloroquine induces apoptosis of MPM cells if associated with nutritional stress [36] or
402 PI3K/mTOR inhibition [20], two conditions that induce ER stress [15, 16, 37], suggesting that at
403 least part of the pro-apoptotic effect of chloroquine is triggered by ER dysfunctions. Since
404 carfilzomib and chloroquine act downstream the ubiquitination system and prevent the degradation
405 of ubiquitinated proteins by proteasome and lysosomes [24], these drugs may produce an "action
406 mass"-like effect: by blocking the degradation of ubiquitinated LIP *via* proteasome and lysosomes,
407 carfilzomib and chloroquine increased the amount of ubiquitinated LIP to a level saturating the
408 ubiquitination capacity of MPM cells. This saturation ultimately resulted in the accumulation of
409 not-ubiquitinated LIP that triggered the CHOP/TRIB3/caspase 3 pro-apoptotic pathway.
410 In addition to ER stress-linked pro-apoptotic mechanisms, carfilzomib and chloroquine are known
411 ICD inducers [12, 38].

Until now, synergistic anti-tumor effects exerted by combining proteasome and lysosome inhibitors with platinum derivatives [33, 35, 39] were reported only *in vitro*. Our study is the first one demonstrating that the combination treatment of carfilzomib, chloroquine and cisplatin is effective in preclinical models of cisplatin-resistant MPM, by inducing ER stress-dependent apoptosis and activating the host immune system against MPM. Such triple combination did not elicit detectable signs of systemic toxicity *in vivo*. Moreover, each agent used in our preclinical model has well-known pharmacodynamic, pharmacokinetic and toxicological profiles for the extensive clinical use. These considerations are encouraging in the perspective of translating the triple combination cisplatin, carfilzomib and chloroquine to clinical settings.

## Conclusions

Our work demonstrates that LIP levels strongly correlated with MPM response to cisplatin *in vitro*, providing the preliminary data to evaluate if the correlation between high LIP ubiquitination and low survival is valid in larger patients cohort. If the data reported in this study was confirmed, LIP ubiquitination may represent a factor predictive of clinical response to cisplatin. We suggest to include pharmacological inhibitors of LIP degradation, such as a combination of proteasome and lysosome inhibitors, in the number of strategies under evaluation to improve the response of MPM to the current treatment.

## Data availability

All data generated or analysed during this study are included in this published article and its supplementary information files.

## Conflict of interests

None.

## Funding

438 This work was supported by Italian Association for Cancer Research (IG15232 to CR), Italian
439 Ministry of University and Research (EX60% Funding 2015 to SN and CR); Italian Ministry of
440 Health (to LR and GVS); De Benedetti-Cherasco Foundation (Torino-Weizmann Collaborative
441 Program: Scientific Cooperation and Exchange to MR and CR); Fondazione Cassa di Risparmio di
442 Torino (to CR). ICS is recipient of PhD scholarships from the Italian Institute for Social Security
443 (INPS). VM is a PhD fellow of Erasmus Mundus-ERAWEB Action 2 program.
444 The funding institutions had no role in the study design, data collection and analysis, or in writing
445 the manuscript.
446

447 **References**

448 [1] S. Remon, N. Reguart, J. Corral, P. Lianes, Malignant pleural mesothelioma: new hope in the
449 horizon with novel therapeutic strategies. Cancer Treat. Rev. 41 (2015) 27-34.
450 [2] M.A. Bonelli, C. Fumarola, S. La Monica, R. Alfieri, New therapeutic strategies for malignant
451 pleural mesothelioma. Biochem. Pharmacol. 123 (2017) 8-18.
452 [3] V. Izzi, L. Masuelli, I. Tresoldi, C. Foti, A. Modesti, R. Bei, Immunity and malignant
453 mesothelioma: from mesothelial cell damage to tumor development and immune response-based
454 therapies. Cancer Lett. 322 (2012) 18-34.
455 [4] L.A. Lievense, K. Bezemer, R. Cornelissen, M.E. Kaijen-Lambers, J.P. Hegmans, J.G. Aerts,
456 Precision immunotherapy; dynamics in the cellular profile of pleural effusions in malignant
457 mesothelioma patients. Lung Cancer 107 (2017) 36-40.
458 [5] S. Khanna, A. Thomas, D. Abate-Daga, J. Zhang, B. Morrow, S.M. Steinberg, et al., Malignant
459 Mesothelioma Effusions Are Infiltrated by CD3(+) T Cells Highly Expressing PD-L1 and the PD-
460 L1(+) Tumor Cells within These Effusions Are Susceptible to ADCC by the Anti-PD-L1 Antibody
461 Avelumab. J. Thorac. Oncol. 11 (2016) 1993-2005.

462 [6] M.M. Awad, R.E. Jones, H. Liu, P.H. Lizotte, E.V. Ivanova, M. Kulkarni, et al., Cytotoxic T
463 Cells in PD-L1-Positive Malignant Pleural Mesotheliomas Are Counterbalanced by Distinct
464 Immunosuppressive Factors. Cancer Immunol. Res. 4 (2016) 1038-1048.
465 [7] J.G. Aerts, L.A. Lievense, H.C. Hoogsteden, J.P Hegmans, Immunotherapy prospects in the
466 treatment of lung cancer and mesothelioma. Transl. Lung Cancer Res. 3 (2014) 34-45.
467 [8] R.A. Stahel, W. Weder, E. Felley-Bosco, U. Petrausch, A. Curioni-Fontecedro, I. Schmitt-Opitz,
468 et al., Searching for targets for the systemic therapy of mesothelioma. Ann. Oncol. 26 (2015) 1649-
469 1660.
470 [9] D.A. Fennell, Y. Summers, J. Cadranel, T. Benepal, D.C. Christoph, R. Lal, et al., Cisplatin in
471 the modern era: The backbone of first-line chemotherapy for non-small cell lung cancer. Cancer
472 Treat. Rev. 44 (2016) 42-50.
473 [10] S.E. Farber-Katz, H.C. Dippold, M.D. Buschman, M.C. Peterman, M. Xing, C.J. Noakes, et al.,
474 DNA damage triggers Golgi dispersal via DNA-PK and GOLPH3. Cell. 2014;156: 413-427.
475 [11] A. Mandic, J. Hansson, S. Linder, M. Shoshan, Cisplatin induces endoplasmic reticulum stress
476 and nucleus-independent apoptotic signaling. J. Biol. Chem. 278 (2003) 278 9100-9106.
477 [12] L. Galluzzi, A. Buqué, O. Kepp, L. Zitvogel, G. Kroemer, Immunogenic cell death in cancer
478 and infectious disease. Nat. Rev. Immunol. 7 (2017) 97-111.
479 [13] C. Riganti, B. Castella, J. Kopecka, I. Campia, M. Coscia, G. Pescarmona, et al., Zoledronic
480 acid restores doxorubicin chemosensitivity and immunogenic cell death in multidrug-resistant
481 human cancer cells. PLoS One. 8 (2013) e60975.
482 [14] C. Riganti, M.F. Lingua, I.C. Salaroglio, C. Falcomatà, L. Righi, D. Morena, et al.,
483 Bromodomain inhibition exerts its therapeutic potential in malignant pleural mesothelioma by
484 promoting immunogenic cell death and changing the tumor immune-environment.
485 Oncoimmunology. 7 (2017) e1398874.
486 [15] I. Kim, W. Xu, J. Reed, Cell death and endoplasmic reticulum stress: Disease relevance and
487 therapeutic opportunities. Nat. Rev. Drug Discov. 7 (2008) 1013-1030.

488 [16] E. Chevet, C. Hetz, A. Samali, Endoplasmic reticulum stress-activated cell reprogramming in
489 oncogenesis. Cancer Discov. 5 (2015) 586-597.
490 [17] O. Meir, E. Dvash, A. Werman, M. Rubinstein, C/ebp-beta regulates endoplasmic reticulum
491 stress-triggered cell death in mouse and human models. PLoS One. 5 (2010) e9516.
492 [18] C. Chiribau, F. Gaccioli, C. Huang, C. Yuan, M. Hatzoglou, Molecular symbiosis of chop and
493 c/ebp beta isoform lip contributes to endoplasmic reticulum stress-induced apoptosis. Mol. Cell.
494 Biol. 30 (2010) 3722-3731.
495 [19] N. Ohoka, S. Yoshii, T. Hattori, K. Onozaki, H. Hayashi, Trb3, a novel er stress-inducible gene,
496 is induced via atf4-chop pathway and is involved in cell death. EMBO J. 24 (2005) 1243-1255.
497 [20] C. Riganti, J. Kopecka, E. Panada, S. Barak, M. Rubinstein, The role of C/EBP-β LIP in
498 multidrug resistance. J. Natl. Cancer Inst. 107 (2015) piidjv046.

499 [21] S. Doublier, D.C. Belisario, M. Polimeni, L. Annaratone, C. Riganti, E. Allia, et al., HIF-1
500 activation induces doxorubicin resistance in MCF7 3-D spheroids via P-glycoprotein expression: a
501 potential model of the chemo-resistance of invasive micropapillary carcinoma of the breast. BMC
502 Cancer. 12 (2012) e4.
503 [22] M. Obeid, A. Tesniere, F. Ghiringhelli, G.M. Fimia, L. Apetoh, J.L. Perfettini, et al.,
504 Calreticulin exposure dictates the immunogenicity of cancer cell death. Nat. Med. 13 (2007) 54-61
505 [23] J. Zhou, S-H. Tan, V. Nicolas, C. Bauvy, N-D. Yang, J. Zhang, et al., Activation of lysosomal
506 function in the course of autophagy via mTORC1 suppression and autophagosome-lysosome
507 fusion. Cell Res. 23 (2013) 508-523.
508 [24] I. Dikic, Proteasomal and Autophagic Degradation Systems. Annu. Rev. Biochem. 86 (2017)
509 193-224.
510 [25] Y-T. Wu, H-L. Tan, G. Shui, C. Bauvy, Q. Huang, M.R. Wenk, et al., Dual Role of 3-
511 Methyladenine in Modulation of Autophagy via Different Temporal Patterns of Inhibition on Class
512 I and III Phosphoinositide 3-Kinase. J. Biol. Chem. 285 (2010) 10850-10861.

513 [26] N. Echeverry, G. Ziltener, D. Barbone, W. Weder, R.A. Stahel, V.C. Broaddus, et al.,
514 Inhibition of autophagy sensitizes malignant pleural mesothelioma cells to dual PI3K/mTOR
515 inhibitors. Cell Death Dis. 6 (2015) e1757.
516 [27] Y. Li, E. Bevilacqua, C.B. Chiribau, M. Majumder, C. Wang, C.M Croniger, et al., Differential
517 control of the ccaat/enhancer-binding protein beta (c/ebp beta) products liver-enriched transcriptional
518 activating protein (lap) and liver- enriched transcriptional inhibitory protein (lip) and the regulation
519 of gene expression during the response to endoplasmic reticulum stress. J. Biol. Chem. 283 (2008)
520 22443-22456.
521 [28] M.M. Gottesman, T. Fojo, S.E. Bates, Multidrug resistance in cancer: role of ATP-dependent
522 transporters. Nat. Rev. Cancer. 2 (2002) 48-58.
523 [29] A. Tesniere, F. Schlemmer, V. Boige, O. Kepp, I. Martins, F. Ghiringhelli, et al., Immunogenic
524 death of colon cancer cells treated with oxaliplatin. Oncogene. 29 (2010) 482-491.
525 [30] E. Beyranvand Nejad, T.C. van der Sluis, S. van Duikeren, H. Yagita, G.M. Janssen, P.A. van
526 Veelen, et al., Tumor Eradication by Cisplatin Is Sustained by CD80/86-Mediated Costimulation of
527 CD8+ T Cells. Cancer Res. 76 (2016) 6017-6029.
528 [31] S. Di Blasio, I.M. Wortel, D.A. van Bladel, L.E. de Vries, T. Duiveman-de Boer, K. Worah, et
529 al., Human CD1c(+) DCs are critical cellular mediators of immune responses induced by
530 immunogenic cell death. Oncoimmunology. 5 (2016) e1192739.
531 [32] I. Martins, O. Kepp, F. Schlemmer, S. Adjemian, M. Tailler, S. Shen, et al., Restoration of the
532 immunogenicity of cisplatin-induced cancer cell death by endoplasmic reticulum stress. Oncogene.
533 30 (2011) 1147-1158.
534 [33] A.C. Borczuk, C.G.A. Cappellini, H.K. Kim, M. Hesdorffer, R.N. Taub, C.A. Powell,
535 Molecular profiling of malignant peritoneal mesothelioma identifies the ubiquitin–proteasome
536 pathway as a therapeutic target in poor prognosis tumors. Oncogene. 26 (2007) 610-617.

[34] C. Follo, C. Barbone, W.G. Richards, R. Bueno, V.C. Broaddus, Autophagy initiation correlates with the autophagic flux in 3D models of mesothelioma and with patient outcome. Autophagy. 12 (2016) 1180-1194.

[35] G.J. Gordon, M. Mani, G. Maulik, L. Mukhopadhyay, B.Y. Yeap, H.L. Kindler, et al., Preclinical studies of the proteasome inhibitor bortezomib in malignant pleural mesothelioma. Cancer Chemother. Pharmacol.61 (2008) 549-558.

[36] S. Battisti, D. Valente, L. Albonici, R. Bei, A. Modesti, C. Palumbo, Nutritional Stress and Arginine Auxotrophy Confer High Sensitivity to Chloroquine Toxicity in Mesothelioma Cells. Am. J. Respir. Cell. Mol. Biol. 46 (2012) 498-506.

[37] C. Appenzeller-Herzog, M.N. Hall, Bidirectional crosstalk between endoplasmic reticulum stress and mTOR signaling. Trends Cell. Biol. 22 (2012) 274-282.

[38] A.M. Dudek, A.D. Garg, D.V. Krysko, D. De Ruysscher, P. Agostinis, Inducers of immunogenic cancer cell death. Cytokine Growth Factor Rev. 24 (2013) 319-333.

[39] Y-J. Lee, G.J. Lee, S.S. Yi, S-H. Heo, C-R. Park, H-S. Nam, et al., Cisplatin and resveratrol induce apoptosis and autophagy following oxidative stress in malignant mesothelioma cells. Food Chem. Toxicol. 97 (2016) 96-107.

**Figure legends**

**Figure 1. Ubiquitination of LIP correlates with cisplatin resistance in mesothelioma**

**a.** Levels of *C/EBPβ* mRNA as determined by qRT-PCR in triplicates, in 3 primary human non-transformed mesothelial cells (HMC) and 9 primary human malignant pleural mesothelioma (MPM) samples. Epi: epithelioid; Bip: biphasic; Sar: sarcomatous. **b.** Expression and ubiquitination of C/EBP-β LAP and LIP in HMC and MPM samples. Whole cell lysate was immunoprecipitated (IP) with anti C/EBP-β antibody that recognize the common C-terminus C/EBP-β - i.e. either LIP or LAP - and the blot was probed (IB) with the anti C/EBP-β antibody, to detect total levels of C/EBP-β LAP and LIP isoforms, or with an anti-mono/poly-ubiquitin antibody, to detect the corresponding

ubiquitinated forms. *Upper-middle panels, last lane*: control immunoblot of MPM1 cell extract immunoprecipitated in the absence of antibody. Arrow, *middle panel*: ubiquitinated LIP, according to the expected molecular weight. Before immunoprecipitation, an aliquot of cell lysate was probed with an anti-β-tubulin antibody, to check that equal amounts of proteins from each extract were loaded in immunoprecipitation. The figure is representative of 1 out of 3 experiments. **c.** The mean band density of ubiquitinated LIP (indicated by the arrow, *middle panel*, Figure 1b) and the mean band density of total LIP (*upper panel*, Figure 1b) was calculated with the ImageJ software and expressed as arbitrary optical density units, setting the mean ratio between ubiquitinated LIP/total LIP in HMC to 1. Data are presented as means±SD (n=3). MPM vs HMC cells: *p<0.001. **d.** Correlation between $IC_{50}$ of cisplatin (Pt; Supplementary Table 3) and LIP ubiquitination, calculated with the ImageJ software . The mean band density of ubiquitinated LIP (indicated by the arrow, Figure 1b) was expressed as arbitrary optical density units, setting the mean band density in HMC samples to 1 (Supplementary Table 4a). **e-f.** LIP ubiquitination (indicated by the arrow, Figure 1b) was ranked according to mean band density of each patient (Supplementary Table 4a), and median value was calculated. Patients were classified as "LIP low" if LIP ubiquitination was higher or equal to the median value (n=5, i.e. patient 3, 4, 7,8, 9), "LIP high" if LIP ubiquitination was lower or equal to the median value (n=4, i.e. patient 1, 2, 5, 6). Progression free survival (panel **e**) and overall survival (panel **f**) probability was calculated using the Kaplan-Meier method. LIP high vs. LIP low group:*p<0.03 (panel **e**); *p<0.01 (panel **f**). UQ-LIP: ubiquitinated LIP

**Figure 2. LIP reconstitution induces apoptosis and rescues cisplatin-cytotoxicity in mesothelioma**

**a.** Immunoblot of the indicated proteins in extracts of MPM1 (epithelioid MPM) and MPM7 (sarcomatous MPM) cells, stably transfected with the doxycycline-inducible LIP-expression vector, cultured in the absence (-, Ctrl) or presence (+) of cisplatin (Pt, 25 μM) and doxycycline for 24 h. The figure is representative of 1 out of 3 experiments. **b**. Cell cycle analysis of cells treated as in **a**, performed by flow cytometry in duplicates. Pooled data of MPM 1-9 as means±SD (n=3). LIP-

589 treated vs. Ctrl cells:*p<0.01; LIP+Pt-treated cells vs. Pt-treated cells:°p<0.001. **c.** Cell proliferation
590 in cultures treated 8 h after seeding (time "0" in the graph) as in **a**. Pooled data of MPM 1-9 as
591 means±SD (n=4). LIP-treated vs. Ctrl cells (72-96 h):*p<0.01; LIP+Pt-treated cells vs. Pt-treated
592 cells (72-96 h):°p<0.001. **d**. Representative photographs of cells stained with crystal violet (96 h;
593 *left panel*) and quantitation of crystal violet-stained cells, expressed as percentage of viable cells
594 compared to untreated cells (*right panel*). Data of MPM1 and MPM7 cells are presented as
595 means±SD (n=4). Pt-treated vs. Ctrl cells:$^{\#}$p<0.05; LIP-treated vs. Ctrl cells:*p<0.001; LIP/LIP+Pt-
596 treated cells vs. Pt-treated cells:°p<0.001.

597 **Figure 3. LIP restoration primes mesothelioma cells for immunogenic cell death**

598 **a.** Immunoblot of C/EBPβ LAP and LIP in whole cell lysates of MPM1 and MPM7 cells,
599 transfected with the inducible expression vector for LAP (*left panel*) or LIP *(right pane*), cultured in
600 the absence (-, Ctrl) or presence (+) of doxycycline (Doxy). The figure is representative of 1 out of
601 3 experiments. **b**. ChIP showing the binding of LAP or LIP to the calreticulin (*CRT*) promoter (site
602 831-843). Bl: blank; DNA input: genomic DNA. The figure is a representative of 1 out of 3
603 experiments. **c.** Levels of calreticulin (*CRT*) mRNA as determined by qRT-PCR in triplicates.
604 Pooled data of MPM 1-9 as means±SD (n=3). LIP-expressing cells vs. un-induced cells:*p<0.001.
605 **d.** Surface calreticulin (CRT) as detected by flow cytometry in duplicates. The histograms represent
606 the results obtained on MPM1 and MPM7. **e**. Phagocytic index of MPM cells phagocytized by DC,
607 as determined by flow cytometry. Pooled data of MPM 1-9 as means±SD (n=3). LIP-expressing
608 cells vs. un-induced cells:*p<0.001. **f.** Percentage of $CD8^{+}CD107^{+}$T-lymphocytes as determined by
609 flow cytometry in duplicates. Pooled data of MPM 1-9 as means±SD (n=3). LIP-expressing cells
610 vs. un-induced cells:*p<0.001. **g.** IFN-γ levels in the supernatant of $CD8^{+}CD107^{+}$T-cells, measured
611 in duplicates. Pooled data of MPM 1-9 as means±SD (n=3). LIP-expressing cells vs. un-induced
612 cells:*p< 0.001.

613 **Figure 4. LIP overcomes cisplatin-resistance and immune-resistance *in vivo***

**a.** $1\times10^7$ AB1 inducibly expressing LIP (clone 1, Supplemnetary Figure 3) were injeted s.c. in 6-weeks-old female immune-competent or immune-deficient (nude) balb/C mice. When tumor reached the volume of 50 $mm^3$, animals (n=10/group) were randomized and treated on days 1,7 and 14 as follows: 1) control (Ctrl) group, treated with 0.1 ml saline solution intravenously (i.v.); 2) LIP group, treated with 1 mg/ml doxycycline in the drinking water to induce the LIP intratumorally; 3) cisplatin (Pt) group, treated with 5 mg/kg cisplatin i.v.; 4) LIP+cisplatin (LIP+Pt) group, treated with cisplatin and doxycycline to induce LIP. Data are means±SD. Pt/LIP+Pt groups vs. Ctrl group (days 15-21:immune-competent mice, day 21:immune-deficient/nude mice):*$p<0.001$; LIP+Pt group vs. Pt group (days 9-21:immune-competent and immune-deficient/nude mice):°$p<0.001$; LIP+Pt group vs. LIP group (days 9-21: immune-competent and immune-deficient/nude mice):$^{\#}p<0.005$; LIP+Pt group in immunocompetent vs. immune-deficient/nude mice: $p<0.005$ (not shown). **b**. Immunoblotting of C/EBPβ LAP and LIP from tumor extracts, to check LIP induction in mice treated with doxycycline. The figure is representative of extracts from two immune-deficient mice and two immune-competent mice. β-tubulin was used as control of equal protein loading. **c.** Sections of tumors from each group of immune-competent animals, stained with hematoxylin and eosin (HE; 20X objective; bar=100 µm), or immunostained with the indicated antibodies (63X objective; bar=10 µm). The photographs are representative of sections from 5 tumors/group. Data are means±SD. Pt/LIP+Pt groups vs. Ctrl group:*$p<0.005$; LIP+Pt group vs. Pt group:°$p<0.001$; LIP+Pt group vs. LIP group:$^{\#}p<0.05$. **d.** Percent of DC cells in tumors grown in immune-competent mice, treated by Pt, doxycycline (LIP) or their combination. The percent of DC was determined in duplicates by flow cytometry of single cell suspensions. **e**. Percent of $CD3^+CD8^+$T-lymphocytes measured as in **d**. Data of panels **d** and **e** are means±SD. Pt/LIP+Pt groups vs. Ctrl group:*$p<0.001$; LIP+Pt group vs. Pt group:°$p<0.001$; LIP+Pt group vs. LIP group:$^{\#}p<0.02$. **f.** IFN-γ levels as measured in duplicates in the supernatant of tumor-draining lymph nodes of immune-competent mice. Data of are means±SD. Pt/LIP+Pt groups vs. Ctrl group:*$p<0.001$; LIP+Pt group vs. Pt group:°$p<0.001$; LIP+Pt group vs. LIP group:$^{\#}p<0.05$.

**Figure 5. LIP undergoes proteasomal and lysosomal degradation in mesothelioma cells**

**a.** Proteasome activity as analyzed in 3 primary HMC and 9 primary human MPM samples, determined in duplicates by a chemiluminescence-based assay. Data are means±SD (n=3). MPM vs. HMC:*p<0.001. **b.** Autophagy activity as measured spectrofluorimetrically in duplicates. Data are means±SD (n=3). MPM vs HMC: *p<0.001. **c.** Lysosome activity as measured in duplicates by a spectrophotometric assay. Data are means±SD (n=3). MPM vs HMC:*p<0.001. **d.** Immunoblot of the indicated proteins in extracts of MPM1 and MPM7 cells, grown for 24 h in the absence (-), or presence of the proteasome inhibitor carfilzomib (20 nM, Ca), the lysosome inhibitor chloroquine (10 μM, Cq), or their combination, with or without, cisplatin (Pt, 25 μM), added for additional 24 h. The effects induced by cisplatin alone are reported in Figure 2a. The figure is representative of 1 out of 3 experiments.

**Figure 6. Carfilzomib and chloroquine rescue cisplatin anti-tumor effects *in vitro* and *in vivo***

**a.** Growth curves of MPM cells, treated 8 h (time "0" in the graph) after seeding with fresh medium (Ctrl), or media containing carfilzomib (20 nM, Ca), chloroquine (10 μM, Cq), or their combination, without or with cisplatin (Pt, 25 μM). The effects induced by cisplatin alone are reported in Figure 2c. Pooled data of MPM 1-9 as means±SD (n=4). All drug-treated cells vs. Ctrl cells (72-96 h):*p<0.001; Ca+Cq+Pt cells vs. Ca+Cq cells (72-96 h):°p<0.001. **b**. Representative photographs of cells stained with crystal violet (96 h). **c.** AB1 cells were injected s.c. in 6-weeks-old growth in immune-competent balb/C mice (n=10/group). When tumor reached the volume of 50 $mm^3$, animals (n=10/group) were randomized and treated on days 1, 7 and 14 as follows: 1) control (Ctrl) group, treated with 0.1 ml saline solution intravenously (i.v.); 2) carfilzomib (Ca) group, treated with 5 mg/kg carfilzomib i.v.; 3) chloroquine (Cq), treated with 10 mg/kg chloroquine *per os*; 4) carfilzomib+chloroquine (Ca+Cq) group, treated with both drugs; 5) carfilzomib+chloroquine+cisplatin (Ca+Cq+Pt) group, treated with carfilzomib, chloroquine and 5 mg/kg cisplatin i.v. (24 h after carfilzomib+chloroquine). Data are means±SD. All drug-treated cells vs. Ctrl group:*p<0.001; Ca+Cq+Pt group vs. Ca+Cq group:°p<0.001. **d.** Sections of tumors from

each group, stained with hematoxylin and eosin (HE; 20X objective; bar=100 µm), or immunostained with the indicated antibodies (63X objective; bar=10 µm). The percentage of CHOP- and cleaved caspase 3-positive cells as determined by analyzing sections from 5 mice of each group (110-93 cells/field), using the Photoshop program. "Ctrl" group intensity was taken as 100%. Data are means±SD. Treated groups vs. Ctrl group:*$p<0.002$; Ca+Cq+Pt group vs. Ca+Cq group:°$p<0.01$. **e.** Percentage of infiltrating DC in tumors grown in mice that were treated as in **d**. **f.** Percentage of infiltrating $CD3^{+}CD8^{+}$T-lymphocytes in these tumors. Data in panels **e** and **f**, determined in duplicates, are means±SD. All drug-treated groups vs. Ctrl group:*$p< 0.001$; Ca+Cq+Pt group vs. Ca+Cq group:°$p< 0.02$. **g.** IFN-γ levels in the supernatants of tumor-draining lymph nodes. Data determined in duplicates are means±SD. All drug-treated groups vs. Ctrl group: *$p<0.001$; Ca+Cq+Pt group vs. Ca+Cq group:°$p<0.05$.

## Conflict of interests

None.

**Figure 1**

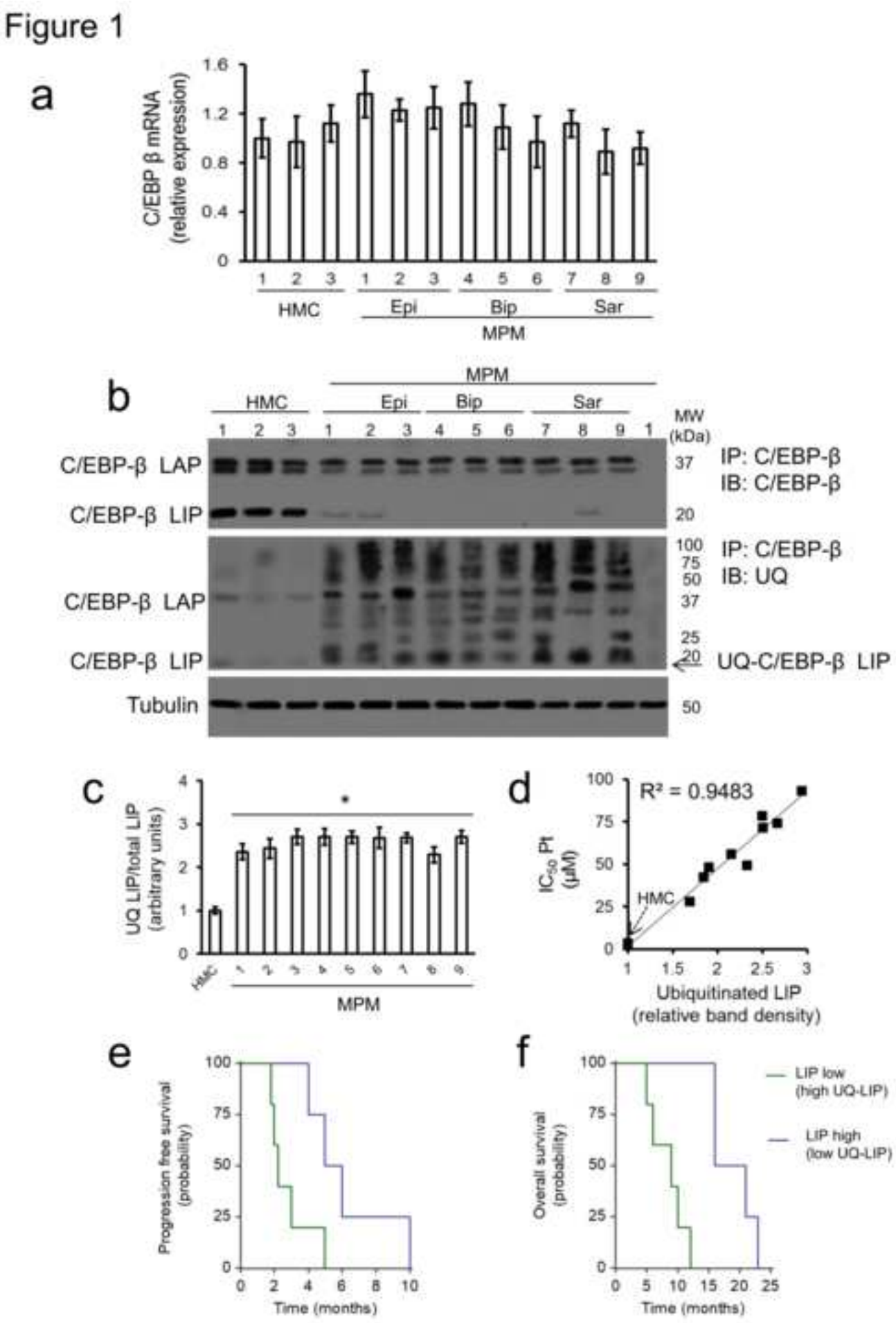
Figure 1
a
C/EBP β mRNA (relative expression)
1.6
1.2
0.8
0.4
0
1 2 3 1 2 3 4 5 6 7 8 9
HMC
Epi
Bip
Sar
MPM
b
MPM
HMC
Epi
Bip
Sar
MW (kDa)
1 2 3 1 2 3 4 5 6 7 8 9 1
C/EBP-β LAP
C/EBP-β LIP
37
20
IP: C/EBP-β
IB: C/EBP-β
100
75
50
37
25
20
IP: C/EBP-β
IB: UQ
C/EBP-β LAP
C/EBP-β LIP
UQ-C/EBP-β LIP
Tubulin
50
c
UQ LIP/total LIP (arbitrary units)
4
3
2
1
0
*
HMC
1 2 3 4 5 6 7 8 9
MPM
d
IC50 Pt (μM)
100
75
50
25
0
R² = 0.9483
HMC
1 1.5 2 2.5 3
Ubiquitinated LIP (relative band density)
e
Progression free survival (probability)
100
75
50
25
0
0 2 4 6 8 10
Time (months)
f
Overall survival (probability)
100
75
50
25
0
0 5 10 15 20 25
Time (months)
LIP low (high UQ-LIP)
LIP high (low UQ-LIP)

Figure 2

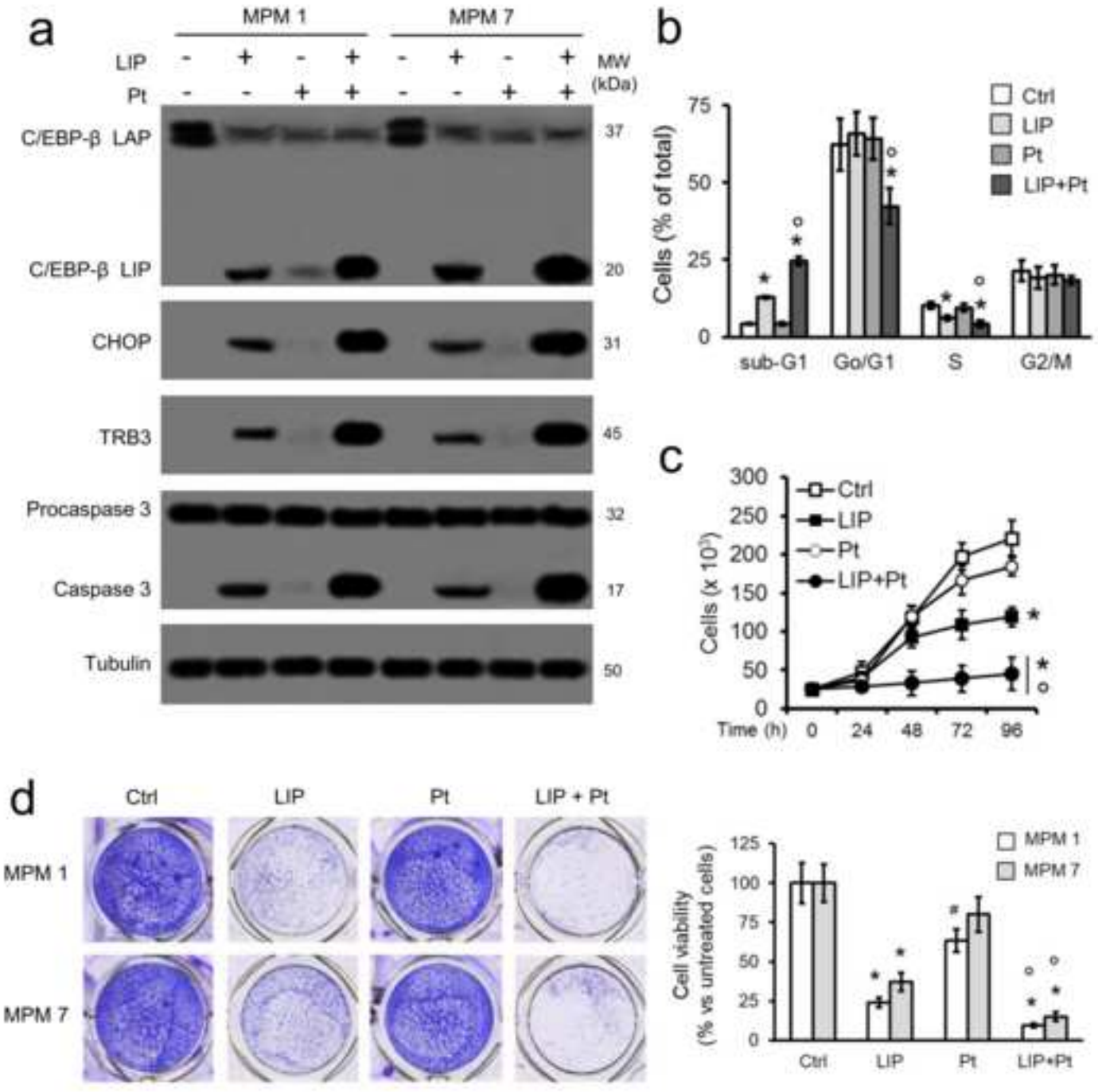
a
MPM 1
MPM 7
LIP
Pt
MW (kDa)
C/EBP-β LAP
C/EBP-β LIP
CHOP
TRB3
Procaspase 3
Caspase 3
Tubulin
37
20
31
45
32
17
50
b
Ctrl
LIP
Pt
LIP+Pt
Cells (% of total)
sub-G1
Go/G1
S
G2/M
c
Cells (x 10³)
Time (h)
d
Ctrl
LIP
Pt
LIP + Pt
MPM 1
MPM 7
Cell viability (% vs untreated cells)

Figure 3

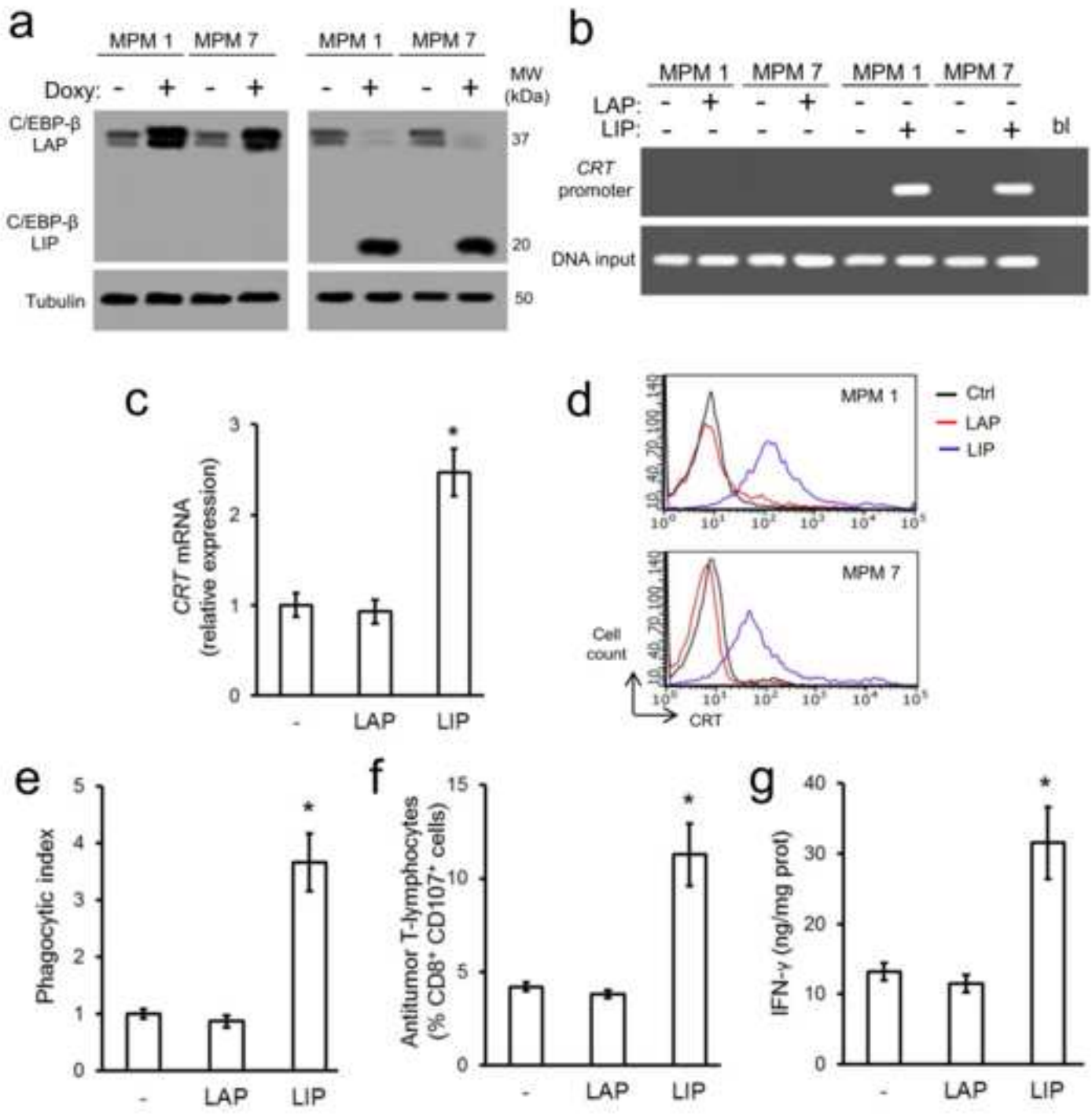
a
MPM 1
MPM 7
MPM 1
MPM 7
Doxy: - + - + - + - +
MW (kDa)
C/EBP-β LAP
C/EBP-β LIP
Tubulin
37
20
50
b
MPM 1
MPM 7
MPM 1
MPM 7
LAP: - + - + - - - -
LIP: - - - - - + - +
bl
CRT promoter
DNA input
c
CRT mRNA (relative expression)
0
1
2
3
*
-
LAP
LIP
d
MPM 1
MPM 7
Ctrl
LAP
LIP
Cell count
CRT
e
Phagocytic index
0
1
2
3
4
5
*
-
LAP
LIP
f
Antitumor T-lymphocytes (% CD8+ CD107+ cells)
0
5
10
15
*
-
LAP
LIP
g
IFN-γ (ng/mg prot)
0
10
20
30
40
*
-
LAP
LIP

**Figure 4**

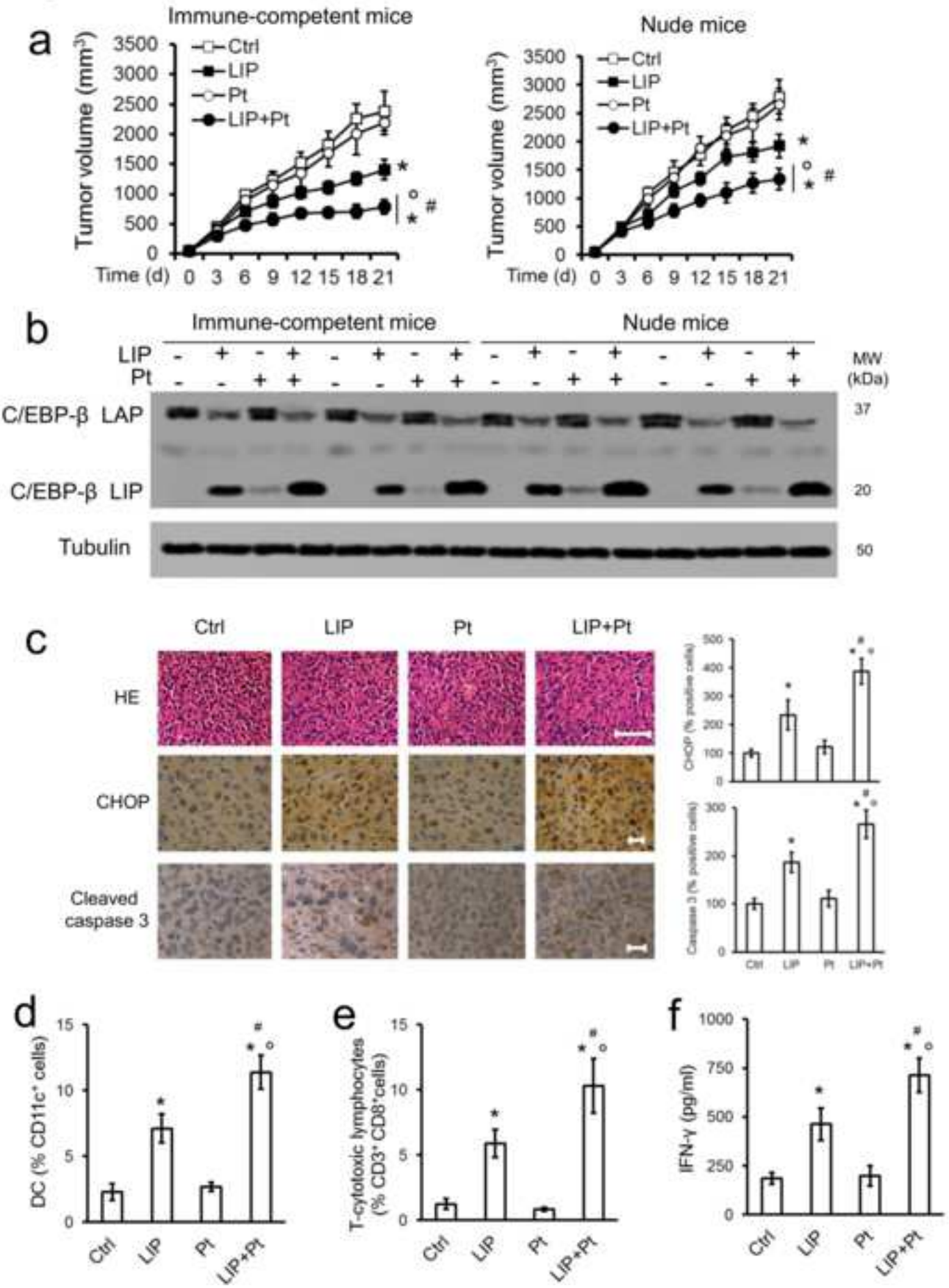
Figure 4
a
Immune-competent mice
Nude mice
Tumor volume (mm3)
Ctrl
LIP
Pt
LIP+Pt
Time (d) 0 3 6 9 12 15 18 21
b
Immune-competent mice
Nude mice
LIP
Pt
MW (kDa)
C/EBP-β LAP
C/EBP-β LIP
Tubulin
37
20
50
c
Ctrl
LIP
Pt
LIP+Pt
HE
CHOP
Cleaved caspase 3
CHOP (% positive cells)
Caspase 3 (% positive cells)
d
DC (% CD11c+ cells)
e
T-cytotoxic lymphocytes (% CD3+CD8+cells)
f
IFN-γ (pg/ml)

**Figure 5**

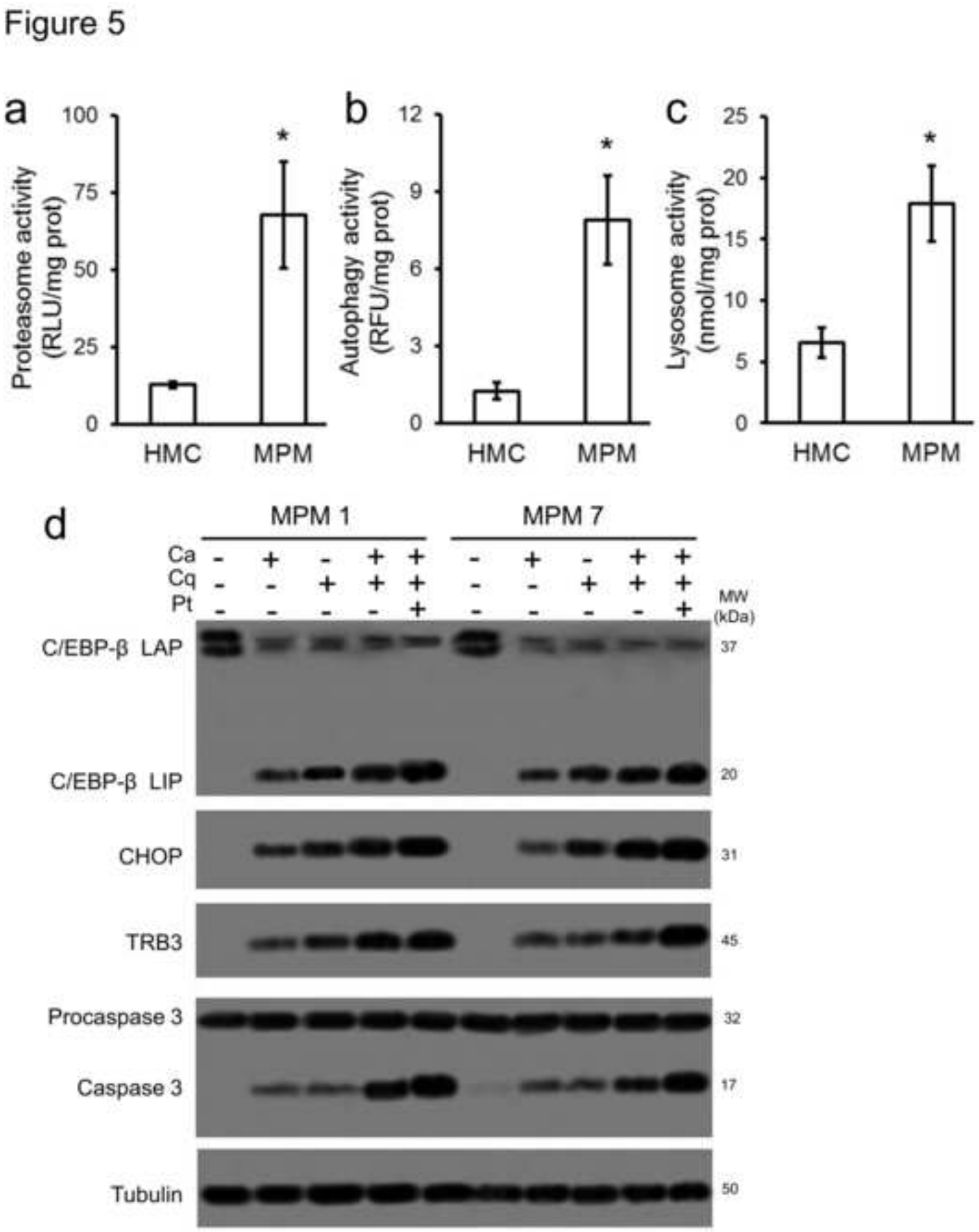
Figure 5
a
Proteasome activity (RLU/mg prot)
100
75
50
25
0
HMC
MPM
b
Autophagy activity (RFU/mg prot)
12
9
6
3
0
HMC
MPM
c
Lysosome activity (nmol/mg prot)
25
20
15
10
5
0
HMC
MPM
d
MPM 1
MPM 7
Ca
Cq
Pt
MW (kDa)
C/EBP-β LAP
C/EBP-β LIP
CHOP
TRB3
Procaspase 3
Caspase 3
Tubulin
37
20
31
45
32
17
50

**Figure 6**

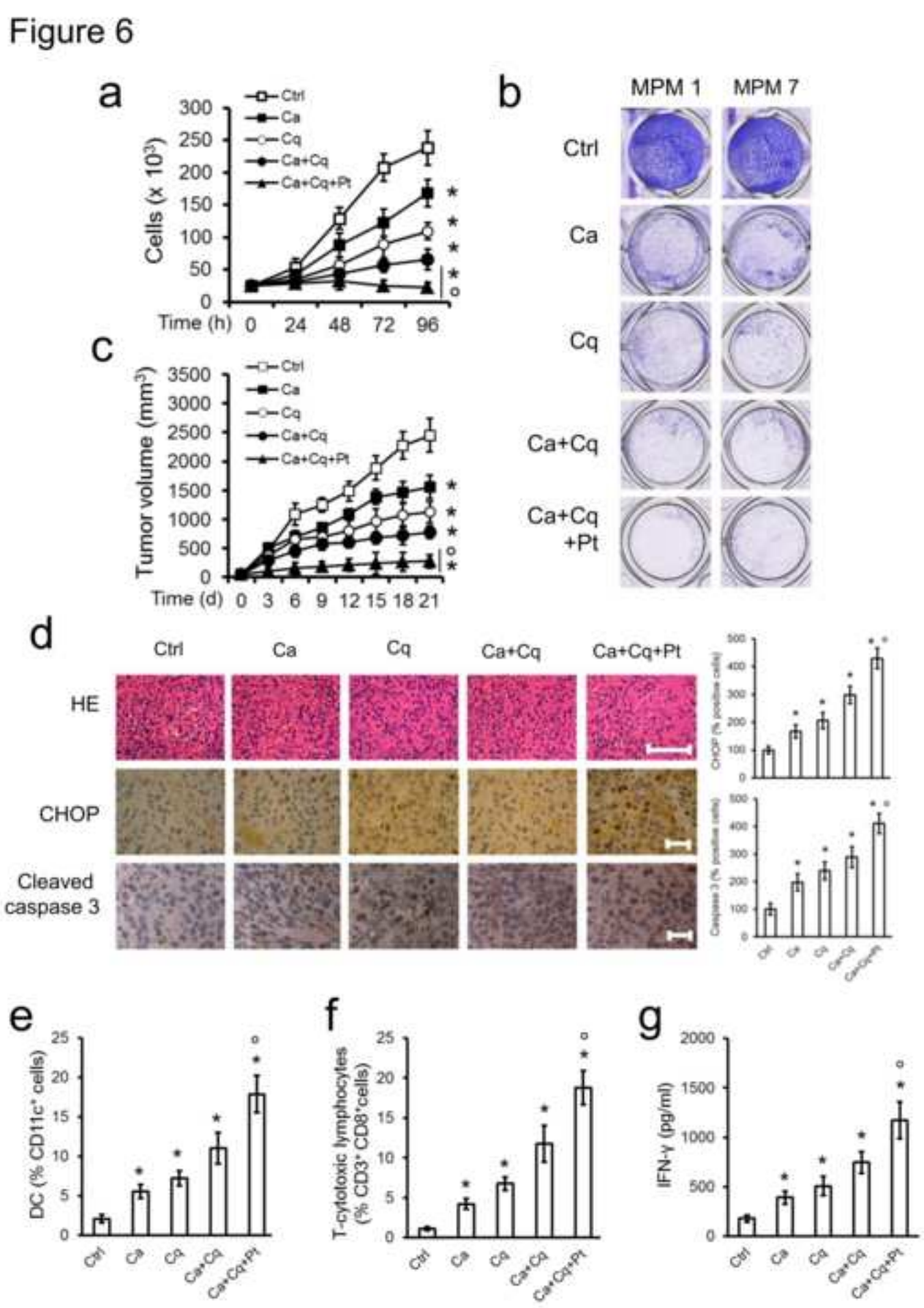
Figure 6
a
Ctrl
Ca
Cq
Ca+Cq
Ca+Cq+Pt
Cells (x 10³)
Time (h) 0 24 48 72 96
b
MPM 1
MPM 7
Ctrl
Ca
Cq
Ca+Cq
Ca+Cq +Pt
c
Tumor volume (mm³)
Time (d) 0 3 6 9 12 15 18 21
d
Ctrl
Ca
Cq
Ca+Cq
Ca+Cq+Pt
HE
CHOP
Cleaved caspase 3
e
DC (% CD11c⁺ cells)
f
T-cytotoxic lymphocytes (% CD3⁺ CD8⁺cells)
g
IFN-γ (pg/ml)

**Supplementary Figure (for online use only)**

**Click here to download Supplementary Figure (for online use only): Supplementary Figures_LC_R1.docx**

## Supplementary Tables

### Supplementary Table 1. Histological characterization of mesothelioma samples

| MPM (UPN) | CALR | PANCK | POD | EMA | CEA | WT1 | CK5 |
|---|---|---|---|---|---|---|---|
| 1 | POS | POS | NEG | NEG | NEG | POS | NEG |
| 2 | POS | POS | NEG | NEG | NEG | POS | NEG |
| 3 | POS | POS | NEG | POS | NEG | POS | NEG |
| 4 | POS | POS | NEG | NEG | NEG | POS | NEG |
| 5 | POS | POS | NEG | NEG | NEG | NEG | NEG |
| 6 | POS | POS | NEG | NEG | NEG | FOC | NEG |
| 7 | NEG | NEG | NEG | NEG | NEG | POS | NEG |
| 8 | FOC | FOC | NEG | NEG | NEG | FOC | NEG |
| 9 | NEG | POS | NEG | NEG | NEG | NEG | NEG |

Results of the immunohistochemical staining of MPM samples for calretinin (CALR), pancytokeratin (PANCK), podoplanin (POD), epithelial membrane antigen (EMA), carcino-embryonic antigen (CEA), Wilms tumor-1 antigen (WT1), cytokeratin 5 (CK5). POS: positive; NEG: negative; FOC: focal positivity. UPN: unknown patient number.

**Supplementary Table 2. Clinical features of mesothelioma patients**

| MPM (UPN) | Histotype | Sex | Age (years) | Asbestos exposure | Surgery | Radiotherapy | First-line chemotherapy with cisplatin | Second-line treatments | Progression free survival (months) | Overall survival (months) |
|---|---|---|---|---|---|---|---|---|---|---|
| 1 | epithelioid | M | 51 | P | No | No | Yes | Gemcitabine Vinorelbine | 4.1 | 23 |
| 2 | epithelioid | M | 77 | P | No | Yes | Yes | Gemcitabine | 10.3 | 16 |
| 3 | epithelioid | F | 47 | E | No | Yes | Yes | Trabectedin | 5 | 12 |
| 4 | biphasic | M | 66 | E | Yes | No | Yes | None | 2 | 9 |
| 5 | biphasic | M | 64 | P | No | No | Yes | Cisplatin +pemetrexed | 5.5 | 16 |
| 6 | biphasic | M | 72 | P | No | No | Yes | Trabectedin | 5.1 | 21 |
| 7 | sarcomatous | F | 87 | ND | No | No | Yes | None | 1.8 | 6 |
| 8 | sarcomatous | M | 69 | E | No | No | Yes | Trabectedin | 2.6 | 10 |
| 9 | sarcomatous | M | 79 | P | No | No | Yes | Trabectedin | 2.2 | 5 |

Histological classification of MPM samples, anagraphic and clinical data of patients. M: male; F: female; P: professional; E: environmental; U: unlikely; ND: not-determined. UPN: unknown patient number. First-line chemotherapy: 5 cycles of cisplatin 75 mg/m$^2$ every 21 days. Progression free survival: survival with stable disease from the beginning of cisplatin therapy. Overall survival: survival from the beginning of cisplatin therapy until patients exitus.

**Supplementary Table 3. $IC_{50}$ of cisplatin**

| Samples | $IC_{50}$ (μM) |
|---|---|
| HMC 1 | 1.43±0.37 |
| HMC 2 | 5.28±0.46 |
| HMC 3 | 3.72±0.11 |
| MPM 1 | 28.14±5.77 * |
| MPM 2 | 55.81±9.28 * |
| MPM 3 | 49.45±8.72 * |
| MPM 4 | 78.26±10.75 * |
| MPM 5 | 42.32±5.18 * |
| MPM 6 | 48.11±11.33 * |
| MPM 7 | 71.34±16.32 * |
| MPM 8 | 74.05±12.15 * |
| MPM 9 | 93.52±16.93 * |

$1\times10^4$ cells were seeded in quadruplicate in 96-well plates, treated for 96 h with cisplatin at scalar concentrations (from $10^{-10}$ to $10^{-3}$M), then stained with Neutral red solution. $IC_{50}$ was calculated with the CompuSyn software. Data are means±SD (n=4). MPM cells vs. each HMC: *$p<0.001$.

## Supplementary Table 4. Quantification of ubiquitinated LIP

| a | Figure 1b | |
|---|---|---|
| condition | UQ LIP | total LIP |
| HMC | 1 | 2.669884 |
| MPM1 | 1.692308 | 0.374548 |
| MPM2 | 2.153846 | 0.37125 |
| MPM3 | 2.333333 | 0.424765 |
| MPM4 | 2.5 | 0.920423 |
| MPM5 | 1.846154 | 0.951585 |
| MPM6 | 1.903846 | 1.055493 |
| MPM7 | 2.50641 | 1.056983 |
| MPM8 | 2.666667 | 1.054902 |
| MPM9 | 2.942308 | 1.046657 |

| b | Figure 2a | |
|---|---|---|
| condition | UQ LIP | total LIP |
| MPM1 Ctrl | 1 | 1 |
| MPM1 LIP | 0.538232 | 0.866023 |
| MPM1 Pt | 0.688645 | 0.851552 |
| MPM1 LIP+Pt | 0.317735 | 0.851552 |
| MPM7 Ctrl | 1 | 1 |
| MPM7 LIP | 0.834996 | 0.834996 |
| MPM7 Pt | 0.604407 | 0.698161 |
| MPM7 LIP+Pt | 0.249762 | 0.687504 |

| c | Figure 5d | |
|---|---|---|
| condition | UQ LIP | total LIP |
| MPM1 Ctrl | 1 | 1 |
| MPM1 Ca | 0.75358 | 1.319789 |
| MPM1 Cq | 0.742566 | 1.14256 |
| MPM1 Ca+Cq | 0.613394 | 1.731273 |
| MPM1 Ca+Cq+Pt | 0.598165 | 2.538498 |
| MPM7 Ctrl | 1 | 1 |
| MPM7 Ca | 0.688755 | 1.256245 |
| MPM7 Cq | 0.690439 | 1.269075 |
| MPM7 Ca+Cq | 0.689884 | 1.748149 |
| MPM7 Ca+Cq+Pt | 0.595311 | 2.464859 |

Band density of ubiquititinated (UQ) LIP and total LIP of the blots reported in Figure 1b (Table **a**), Figure 2a and Supplementary Figure 1a (Table **b**), Figure 5d and Supplementary Figure 7a (Table **c**), was calculated using ImageJ software (http://www.rsb.info.nih.gov/ij/). The ratio between ubiquitinated LIP/total LIP was reported in Figure 1c, Supplementary Figure 1b and Supplementary Figure 7b.

**Supplementary Table 5. Cisplatin sensitization in mesothelioma cells overexpressing LIP**

| MPM (UPN) | $IC_{50}$ (µM) | Sf |
|---|---|---|
| 1 | 8.05 ± 0.23 | 3.49 |
| 2 | 11.23 ± 0.51 | 4.96 |
| 3 | 7.24 ± 0.91 | 6.83 |
| 4 | 8.36 ± 0.15 | 9.36 |
| 5 | 14.23 ± 4.12 | 3.18 |
| 6 | 7.11 ± 0.81 | 6.76 |
| 7 | 10.23 ± 0.85 | 6.97 |
| 8 | 15.63 ± 1.91 | 4.73 |
| 9 | 24.58 ± 3.14 | 3.80 |

$1\times10^4$ cells were seeded in quadruplicate in 96-well plates, treated for 96 h with cisplatin at scalar concentrations (from $10^{-10}$ to $10^{-3}$M), then stained with Neutral red solution. $IC_{50}$ was calculated with the CompuSyn software. Data are presented as means±SD (n=4). $IC_{50}$ in LIP-overexpressing MPM cells vs. wild-type MPM cells (reported in Supplementary Table 3): *$p<0.001$ (not shown in this Table). Sensitization factor (Sf) was obtained by dividing $IC_{50}$ in wild-type MPM cells (Supplementary Table 3) and $IC_{50}$ in LIP-overexpressing cells (Supplementary Table 4).

**Supplementary Table 6. Hematochemical parameters of the animals**

| | Ctrl | Ca | Cq | Ca+Cq | Ca+Cq+Pt |
|---|---|---|---|---|---|
| RBC ($x10^6$/µl) | 13.09±1.88 | 11.72±2.35 | 12.45±3.89 | 11.09±3.78 | 11.38±2.11 |
| Hb (g/dl) | 13.78±2.91 | 12.52±2.18 | 13.21±1.98 | 12.81±2.71 | 12.09±1.93 |
| WBC ($x10^3$/µl) | 13.23±2.81 | 12.21±3.11 | 12.84±2.29 | 13.78±2.11 | 11.83±2.48 |
| PLT ($x10^3$/µl) | 1145±239 | 901±175 | 1093±269 | 1193±207 | 946±152 |
| LDH (U/l) | 5879±982 | 5729±498 | 6230±502 | 6183±529 | 5936±610 |
| AST (U/l) | 187±42 | 229±41 | 173±45 | 179±55 | 209±47 |
| ALT (U/l) | 52±11 | 51±15 | 62±9 | 52±13 | 45±17 |
| AP (U/l) | 126±38 | 101±25 | 136±42 | 145±33 | 121±34 |
| Creatinine (mg/l) | 0.031±0.006 | 0.027±0.005 | 0.034±0.007 | 0.030±0.007 | 0.035±0.006 |
| CPK (U/l) | 345±67 | 411±109 | 398±163 | 372±152 | 361±129 |

Immunocompetent balb/C mice (n=10/group) were treated as described in Figure 6. Blood was collected immediately after euthanasia and analyzed for red blood cells (RBC) counts, hemoglobin (Hb), white blood cells (WBC), platelets (PLT), lactate dehydrogenase (LDH), aspartate aminotransferase (AST), alanine aminotransferase (ALT), alkaline phosphatase (AP), creatinine, creatine phosphokinase (CPK). Data are means±SD.